of the MICA protein [23, 29], which is involved in the susceptibility to hepatocellular carcinoma in chronic hepatitis patients [24, 25], we focused on this miRNA in further analyses.

Efficient delivery of miRNAs into liver cell lines using bionanocapsules

Efficient delivery methods of genes or compounds into targeted tissues or cells are essential to translate the *in vitro* results into clinical settings. Here, we utilized BNCs [21, 30, 31], which were originally developed to deliver genes and drugs with high efficiency and specificity to human liver-derived cells, as an efficient delivery method for miRNAs into human liver cells, including primary hepatocytes. Since BNCs are composed of HBV L proteins, the distribution of these BNCs and infected HBV should be similar. To confirm the efficiency of delivery of miRNAs into liver-derived cells by BNCs, we delivered BNCs carrying let-7g or miRNA93 to the human hepatocellular carcinoma cell lines, Huh7 and HepG2 cells, and to human normal hepatocytes immortalized with SV40 large T antigen, Fa2N4 cells [28]. The day after delivery of the BNCs, cells were collected and subjected to Northern blotting against let-7g, miRNA93, and U6, the loading control, and the results showed successful delivery of miRNAs into all cell lines tested (Figure 2a). The biological function of the delivered miRNAs was confirmed using luciferase-based reporters, which measured let-7g and miRNA93 functions [23]. Huh7 and Hep3B cells transfected with reporter constructs were delivered with let-7g or miRNA93 using BNCs, followed by a luciferase assay at the next day. Delivered miRNAs significantly decreased the corresponding luciferase activity, suggesting that the delivered miRNAs were functioning within the cells (Figure 2b).

We next examined the delivery of miRNAs into 293T cells (human embryonic kidney cell lines) to explore cell-specificity. Only a small increase in miRNA93 expression levels was observed 24 hours after transfer into 293T cells, based on Northern blots (Figure 2c), indicating that the BNCs had high specificity for hepatocyte-derived cells. The expression of transferred miRNA into Huh7 cells could be observed even 3 days after delivery (Figure 2d), suggesting that the delivered miRNAs are expressed

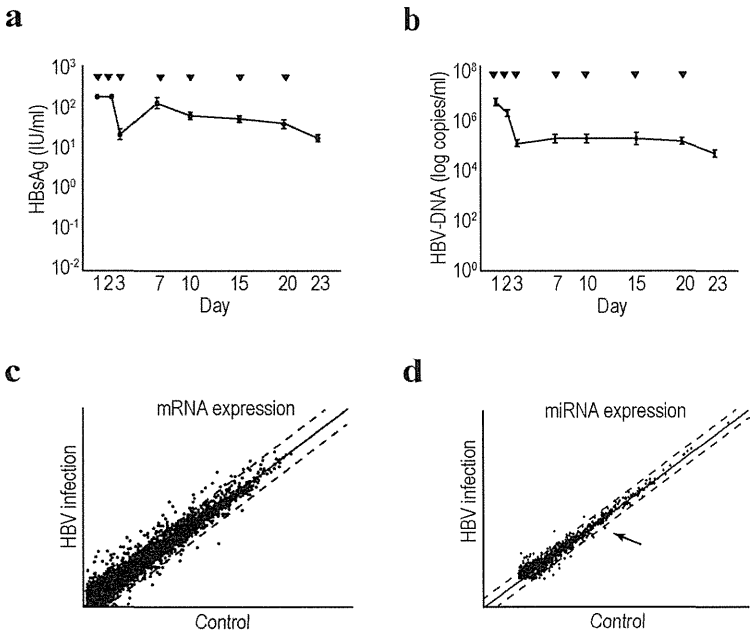

Figure 1: Comprehensive transcriptome and miRNA analyses in HBV-replicating human primary hepatocytes. a, b, Efficient HBV replication in human primary hepatocytes isolated from chimeric mice. Primary human hepatocytes isolated from chimeric mice were seeded into the wells of a 24-well plate. Serum from HBV-infected patients was added to infect the cells with HBV. Media was changed at the indicated days (▼). The supernatant was collected when the media was changed for the analyses of HBsAg levels (a) and HBV-DNA levels (b). Data represent the means ± s.d. of three independent experiments. c, Scatter plot reflecting the transcriptomic results comparing the control and HBV-replicating primary human hepatocytes. Cells at day 7 after HBV infection were used for the analyses. Intensity normalization was performed using global normalization based on the expression levels of all genes analyzed. Dashed lines indicate the thresholds: two-fold increase or 50% decrease in expression levels. The full data are deposited in NCBI GEO database accession: GSE55928. d, A scatter plot of the miRNA microarray results was used to determine the expression levels of comprehensive mature miRNAs. Total RNA from control and HBV-replicating primary hepatocytes at day 7 after infection was used. Dashed lines indicate the thresholds: two-fold increase or 50% decrease in expression levels. Intensity normalization was performed using global normalization based on the expression levels of all miRNAs. The arrow indicates the result for miRNA93. The full data are deposited in NCBI GEO database accession: GSE55929.

for several days.

miRNA delivery into human primary hepatocytes using bionanocapsules

Based on the efficient delivery of miRNA via BNCs into human liver-derived cell lines, we examined the BNC-mediated delivery of miRNAs into non-dividing human primary hepatocytes isolated from chimeric mice, as described above. BNCs could deliver miRNAs efficiently, even into non-dividing human primary hepatocytes, based on Northern blots (Figure 3a), irrespectively of the use of Polybren (Figure 3a).

Since the expression levels of miRNA93 were downregulated by HBV replication (Figure 1d and Supplementary Table 4), we delivered miRNA93 via BNCs into HBV replicating human hepatocytes to rescue the downregulation of miRNA93 levels and examine the effects of decreased miRNA93 on transcript levels (Figure 3b). The rescue of miRNA93 expression, recovered the baseline-level expression of some genes, such as 17-beta-hydroxysteroid dehydrogenase 14 (HSD17B14) and tripartite motif-containing protein 31 (TRIM 31), which

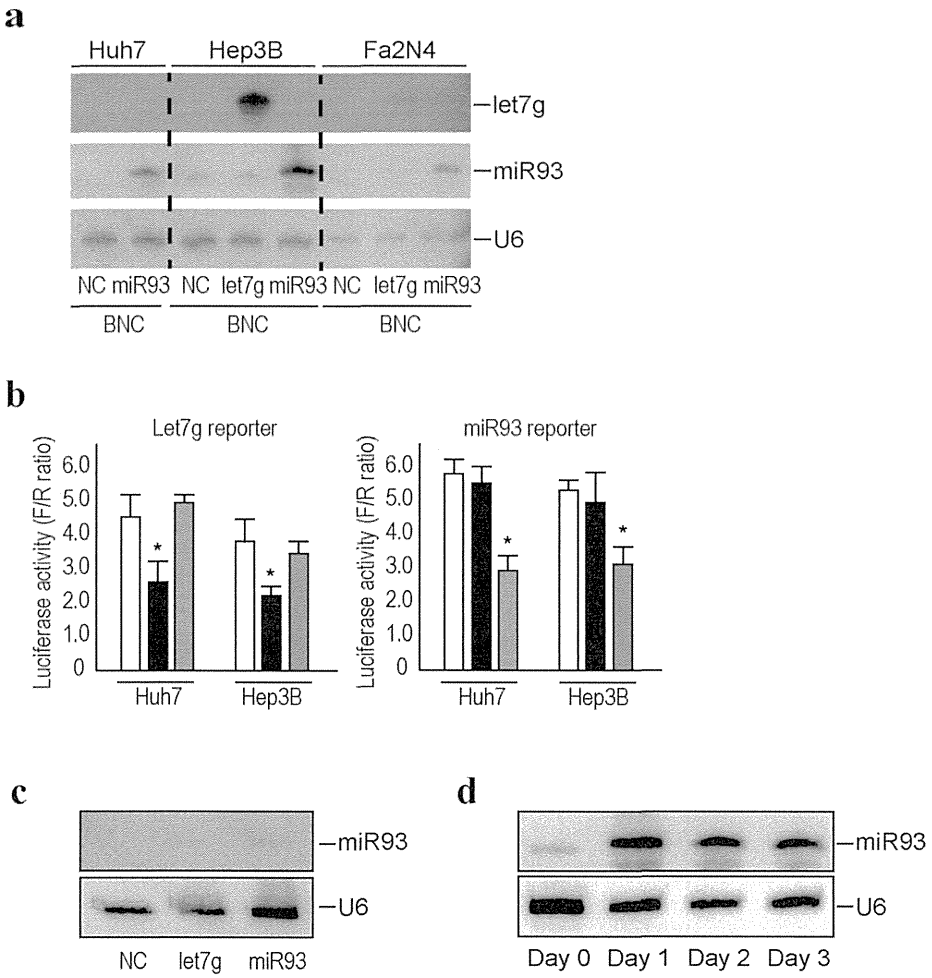

Figure 2: Efficient delivery of miRNAs into liver cell lines using BNCs. a, Northern blotting of miRNAs delivered into liver cells by BNCs. Liver cancer cell lines, Huh7 and Hep3B, and primary hepatocytes immortalized by SV40, Fa2N4, were incubated with BNCs harboring the indicated miRNAs (miRNA93 or let7g) or BNCs without miRNAs (NC). After 24 hours, cells were harvested and subjected to analysis. Membranes were re-probed for let7g, miRNA93, and U6 as a loading control. The results shown are representative of three independent experiments. b, miRNAs delivered using BNCs were biologically functional. Huh7 and Hep3B cells were transfected with the indicated reporter constructs, which indicate the activity of each miRNA function. Twenty-four hours after transfection, cells were mixed with BNCs containing let7g (black bar), miRNA93 (gray bar), or negative control (white bar). Forty-eight hours after transfection, cells were subjected to a dual luciferase assay. Data shown represent the means ± s.d. of the raw ratios (FL/RL), obtained by dividing the firefly luciferase values by the renilla luciferase values, of three independent experiments. $*p < 0.05$. c, Delivery of miRNAs via BNCs were liver cell-specific. The 293T cells (human embryonic kidney cells) were incubated with BNCs containing let7g, miRNA93, or negative control (NC). After 24 hours, cells were subjected to Northern blotting for miRNA93. U6 was used as a loading control. The results shown are representative of two independent experiments. d, miRNA93 expression in Huh7 cells after the delivery of miRNA93 via BNCs. Cells were sequentially collected after incubation with BNCs containing miRNA93 and subjected to Northern blotting. U6 was used as a loading control. The results shown are representative of three independent experiments.

were increased by HBV replication (Supplementary Table 1), suggesting that the mRNA levels of these genes may be directly or indirectly regulated by miRNA93. Although the enhanced decay of target transcripts by miRNAs has been reported [22, 32], miRNAs generally function as translational repressors [33]. However, these miRNA93 delivery results may not be accurate due to direct or indirect effects of miRNA93. In addition, changes in protein levels may differ from our transcript expression results.

Modulation of MICA protein expression levels by delivery of miRNA93 using BNCs

We previously identified miRNA93 as a critical regulator of MICA protein expression [23], which plays a role in the susceptibility to HBV-induced HCC [25]. MiRNA93 regulates MICA protein levels, but not transcript levels [23, 29]. Although it was found that miRNA93 expression levels decreased during HBV replication in primary hepatocytes (Figure 1d and Supplementary Table 4), MICA transcript levels were not affected (GEO accession number: GSE55928), suggesting that the effects of miRNA93 on MICA may be mediated by translational repression and not by mRNA decay, as we reported previously [23]. To confirm changes in the expression level of the MICA protein on the cell surface of primary hepatocytes induced by HBV infection, cells were subjected to FACS analyses. However, the protein expression levels on the cell surface did not change significantly (Figure 4a). MICA is a soluble protein released into the supernatant after shedding by ADAM10 and ADAM17[34]. Our results suggested that the

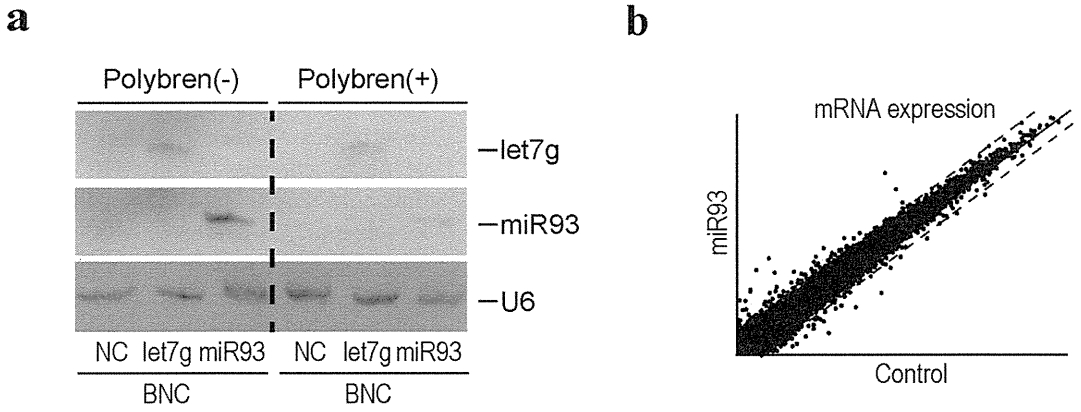

Figure 3: Efficient delivery of functional miRNAs into human primary hepatocytes using BNCs. a, Northern blotting for miRNAs delivered into cells using BNCs. Human primary hepatocytes isolated from chimeric mice were incubated with BNCs containing the indicated miRNAs (miRNA93 or let7g) or BNCs without miRNAs (NC), with or without Polybren. After 24 hours, cells were harvested and subjected to analysis. Membranes were re-probed for let7g, miRNA93, and U6 as a loading control. The results shown are representative of three independent experiments. b, A scatter plot reflecting the transcriptome results between the control and primary human hepatocytes treated with BNCs containing miRNA93. Cells were harvested 24 hours after BNC treatment. Intensity normalization was performed using global normalization based on the expression levels of all genes analyzed. Dashed lines indicate the thresholds: a two-fold increase or 50% decrease in expression levels. The full data are deposited in GEO database accession: GSE55928.

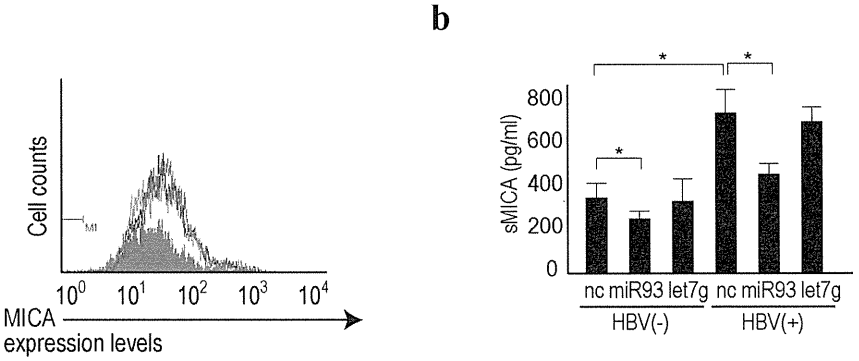

Figure 4: Soluble MICA protein levels were regulated by miRNA93 in human primary hepatocytes. a, Membrane-bound MICA protein expression was not affected by miRNA delivery into human primary hepatocytes. Flow cytometric analysis of membrane-bound MICA protein expression in cells delivered BNC-mediated control (green line), let7g (blue line), or miRNA93 (red line). Gray-shaded histograms represent background staining, assessed using isotype IgG. Representative results from three independent experiments are shown. b, Soluble MICA protein levels in the supernatants of primary hepatocytes after delivery of the indicated miRNAs (let7g or miRNA93) or negative control (NC) with or without HBV replication. Data represent the means ± s.d. of three independent experiments. *p<0.05.

modulated expression of MICA in primary hepatocytes during HBV replication affects this shedding process. To explore this possibility, we examined MICA protein levels in the supernatant using ELISA. As predicted, HBV infection significantly increased the protein concentration of MICA in the supernatant (Figure 4b).

Because an increase in soluble MICA levels in the serum of chronic hepatitis B patients is significantly associated with increased susceptibility to HCC [25], this increase during HBV replication needs to be prevented. Thus, we examined the effects of delivery of BNCs carrying miRNA93 into HBV-infected hepatocytes. Even though the MICA mRNA levels were not significantly affected by miRNA93 delivery based on microarray results (GEO accession: GSE55928), soluble MICA protein in the supernatant significantly decreased according to ELISA (Figure 4b). These results suggested that miRNA93 delivery into the liver decreases soluble MICA levels in the serum, which may be used to prevent HCC in chronic hepatitis B patients.

DISCUSSION

We report that HBV replication in human hepatocytes decreases miRNA93 expression and increases soluble MICA levels. Increased soluble MICA levels in the serum are strongly associated with HBV-related HCC [25], and the increased soluble MICA levels could be antagonized by the delivery of miRNA93 into hepatocytes using BNCs. Thus, BNCs carrying miRNA93 may be used to prevent HCC in patients with chronic HBV infection.

Methods of efficient long-term HBV replication *in vitro* are not commonly available. Although transient transfection assays using fragments or tandem-units of the HBV genome or the full-length HBV genome without vector backbone have been applied [8-12], these models can be analyzed only for short-term replication after transfection. Although stable cell lines carrying HBV genomes are also used, HBV particles are derived from the HBV genome and integrate into the host genome, which differs from natural infection, in which HBV replication mainly relies on HBV cccDNA [6, 7]. Although the most ideal system for HBV infection and replication studies *in vitro* are primary human hepatocytes, they are difficult to obtain. Freshly isolated human hepatocytes from chimeric mice used in this report are relatively easily to obtain, since they proliferate under immune-deficient and liver-damaging conditions. These cells could support HBV replication for a substantial period and are valuable resources for studies on HBV infection and replication.

Another essential tool used in this study is that of BNCs. Primary hepatocytes are generally difficult to transduce with exogenous genes via transfection. Although viral-mediated gene transfer is useful even for primary cells, we chose BNCs as the miRNA delivery method for several reasons. First, since BNCs are composed of HBV L particles, these BNCs preferentially target primary hepatocytes and theoretically target similar cells as does HBV. Second, since we want to develop future therapeutics based on our experimental results, we avoided using viral materials such as lentiviruses or retroviruses to improve biosafety. Third, although BNCs have been established to transfer genes or drugs [21, 31, 35], transfer of miRNAs has not yet been examined, which prompted us to investigate delivery of miRNAs. We found that BNCs could efficiently deliver miRNAs into primary hepatocytes. Although further studies are required, delivery of miRNAs into hepatocytes via BNCs may be a promising approach to target hepatocytes *in vivo*, as BNCs are efficient delivery vehicles in xenograft models using human liver-derived cells [21].

The present results regarding comprehensive transcriptome analyses using HBV replicating hepatocytes may be applicable for future HBV research. While similar experiments are typically performed using transfection in HBV protein-expressing cells, or other relatively artificial experimental settings, the results here may better reflect the *in vivo* situation for HBV-infected hepatocytes. The expression of approximately 0.3% of genes changed during HBV replication when the threshold was set to a greater than 4-fold increase or to less than a 25% decrease. Although some of these genes were consistent with previous transcriptomic studies [36-38], we observed several novel characteristics. First, few inflammation-related genes were included among genes whose expression levels were significantly changed. The reason for this discrepancy remains unclear, but the results were considered accurate, since inflammation is rare when HBV replicates prior to seroconversion in chronic HBV-infected patients. Thus, HBV may be able to evade the sensing system related to innate immunity [39-41]. It should be explored whether changes in HBV sequences or the presence of host cells other than hepatocytes affect gene expression in hepatocytes *in vivo*. Second, based on comprehensive analysis of transcript changes, many CYP-related genes were upregulated during HBV replication, which is consistent with previous reports [27, 28]. Since the biological significance of these changes remain unclear, further studies are required to explore the biological significance during HBV replication.

Microarray analyses of changes in miRNA expression levels in HBV-replicating cells revealed that miRNA expression levels were not affected by HBV replication (2.4% among 2,000 miRNAs when the threshold was set to more than a two-fold increase or less than a 50% decrease). However, the miRNAs whose expression levels changed may play crucial roles in the regulation of target gene expression without affecting transcript expression levels, for example, targeting of the MICA protein by miRNA93, whose expression levels were downregulated by HBV replication. The results of comprehensive miRNA expression level analysis in

HBV-replicating cells may increase our understanding of deregulated gene expression induced by HBV replication in hepatocytes.

MiRNA93 is a critical regulator of MICA protein expression [23, 29]. Thus, the decreased expression of miRNA93 by HBV suggested that the regulation of MICA expression by miRNA93 has biological significance. Polymorphisms in the MICA gene are associated with HBV and HCV-induced HCC [25, 42], and the increase in soluble MICA in the serum can be used as a susceptibility marker for HBV-induced HCC [25]. The increased levels of MICA protein expression agreed with the decreased miRNA93 expression. However, this increase was observed for soluble MICA protein levels and not membrane-bound MICA. While MICA is post-translationally dependent on the cell context or the status of viral infection [34], MICA may be readily processed from the cell surface in HBV-replicating primary hepatocytes and mainly released as soluble protein. Soluble MICA protein may function as a decoy for the NKG2D receptor in immune cells and as an evasion or immune surveillance system during chronic HBV infection. It may also be associated with HBV-induced HCC since HBV-infected hepatocytes may evade from the immune surveillance. Based on these results, BNCs carrying miRNA93 can be used to eliminate HBV-infected hepatocytes, which may be a novel approach for the prevention of subsequent virus-induced HCC.

MATERIALS AND METHODS

Cells

Primary human hepatocytes isolated fresh using the collagenase perfusion method from chimeric uPA/SCID mice with humanized livers [14, 17] were obtained from Phoenix Bio (Hiroshima, Japan). The purity of human hepatocytes was greater than 95%. A total of 3.0×10^5 cells/well were seeded on a type I collagen coated-24-well plate and maintained in DMEM with 10% FBS, 5 ng/ml EGF, 0.25 μg/ml insulin, 0.1 mM ascorbic acid, and 2% DMSO [43]. These cells were able be maintained at a high density for more than 3 weeks, supporting the long-term replication of HBV infection *in vitro*.

HBV infection *in vitro*

Serum from chronically HBV-infected patients with no HBe antibody before seroconversion was used for *in vitro* infection. Serum containing 9.0 log IU/ml of HBV genotype C in a volume of 3 μl, which is approximately 1.5×10^7 copies of HBV, was added to the 3.0×10^5 cells/well, followed by the addition of 4% PEG 8000 at day 0. Cells were washed, and the media was changed at days 1 and 2 and every 5 days thereafter. The media was collected to measure HBsAg and HBV-DNA at days 1, 2, 3, 7, 10, 15, 20 and 23 to confirm HBV replication. Measurements were performed at the clinical laboratory testing company SRL. Inc. (Tokyo, Japan).

cDNA array and miRNA microarray

Human 25K cDNA microarray and human 2K miRNA microarray analyses were performed using miRNA oligo chips according to the standard protocols (Toray Industries, Tokyo, Japan). The data and the experimental conditions were deposited in a public database (GEO: accession numbers: GSE55928 and GSE55929).

Bionanocapsules for miRNA delivery

Hollow particles consisting of HBV L proteins (pre-S1, pre-S2, and S regions) were used as the BNCs, as described previously [20, 21, 30]. The incorporation of miRNAs (miRNA93 or let-7g) into the hollow space and the delivery of miRNAs into human liver cells were performed as described previously [31]. Briefly, 32 μl BNC was added to 1 ml culture media at a final concentration of 50 nM miRNA 24 h before the indicated assays (unless otherwise specified).

Northern blotting of miRNAs

Northern blotting of miRNAs was performed as described previously. Total RNA was extracted using TRIzol Reagent (Invitrogen, Carlsbad, CA, USA) according to the manufacturer's instructions. RNA (10 μg) was resolved on denaturing 15% polyacrylamide gels containing 7 M urea in 1× TBE and then transferred to a Hybond N+ membrane (GE Healthcare) in 0.25× TBE. Membranes were UV-crosslinked and prehybridized in hybridization buffer. Hybridization was performed overnight at 42°C in ULTRAhyb-Oligo Buffer (Ambion) containing a biotinylated probe specific for miRNA93 (CTA CCT GCA CGA ACA GCA CTT TG) and let-7g (AAC TGT ACA AAC TACT ACC TCA), which was heated to 95°C for 2 min prior to hybridization. Membranes were washed at 42°C in 2× SSC containing 0.1% SDS, and the bound probe was visualized using the BrightStar BioDetect Kit (Ambion). Blots were stripped by boiling in a 0.1% SDS, 5 mM EDTA solution for 10 min prior to rehybridization using a U6 probe (CAC GAA TTT GCG TGT CAT CCT T).

Reporter plasmids, transient transfection, and dual luciferase assays

The firefly luciferase reporter plasmid was used to examine let7g and miRNA93 function. pGL4-TK, a renilla luciferase reporter, was used as an internal control [44]. Transfection and dual luciferase assays were performed as described previously [45].

Flow cytometry

The expression levels of MICA on the cell surface were determined using flow cytometry, as described previously [23]. Briefly, cells were hybridized with anti-MICA (1:500; R&D Systems, Minneapolis, MN, USA) and isotype control IgG (1:500; R&D Systems) in 5% BSA/1% sodium azide/PBS for 1 h at 4°C. After washing, cells were incubated with goat anti-mouse Alexa 488 (1:1,000; Molecular Probes, Eugene, OR, USA) for 30 min. Flow cytometry was performed and the data analyzed using Guava Easy Cyte Plus (GE Healthcare, Little Chalfont, UK).

ELISA for MICA

The concentration of MICA in the cell culture supernatant was measured using a sandwich ELISA, according to the manufacturer's instructions (R&D Systems, Minneapolis, MN, USA).

Statistical analysis

Significant differences between groups were determined using the Student's *t*-test when variances were equal and using Welch's *t*-test when variances were unequal. *P*-values less than 0.05 were considered statistically significant.

ACKNOWLEDGMENTS

This work was supported by Grants-in-Aid from the Ministry of Education, Culture, Sports, Science and Technology, Japan (# 25293076 and #24390183) (to M.Otsuka and K.K.); Health Sciences Research Grants from the Ministry of Health, Labour and Welfare of Japan (Research on Hepatitis) (to S.K. and K.K.); the Program for Promotion of Basic and Applied Researches for Innovations in Bio-oriented Industry (BRAIN) (to S.K.); grants from the Okinaka Memorial Institute for Medical Research, the Liver Forum in Kyoto, and the Japanese Society of Gastroenterology (to M.Otsuka).

Editorial note

This paper has been accepted based in part on peer-review conducted by another journal and the authors' response and revisions as well as expedited peer-review in Oncotarget

AUTHOR CONTRIBUTIONS

M.Ohno and M.Otsuka planned the research and wrote the manuscript. M.Ohno, T.K., C.S., T.Y., and A.T. performed the majority of the experiments. R.M., N.K., M.S. and N.K. measured performed ELISA. S.K. provided materials and wrote the manuscript. K.K. supervised the entire project.

COMPETING FINANCIAL INTERESTS

The authors declare no competing financial interests.

REFERENCES

1 Mittal S, El-Serag HB: Epidemiology of hepatocellular carcinoma: Consider the population. J Clin Gastroenterol 2013;47 Suppl:S2-6.

2 Chen DS: From hepatitis to hepatoma: Lessons from type b viral hepatitis. Science 1993;262:369-370.

3 Blachier M, Leleu H, Peck-Radosavljevic M, Valla DC, Roudot-Thoraval F: The burden of liver disease in europe: A review of available epidemiological data. J Hepatol 2013;58:593-608.

4 Yuen MF, Lai CL: Treatment of chronic hepatitis b: Evolution over two decades. J Gastroenterol Hepatol 2011;26 Suppl 1:138-143.

5 Liaw YF, Chu CM: Hepatitis b virus infection. Lancet 2009;373:582-592.

6 Omata M: Treatment of chronic hepatitis b infection. N Engl J Med 1998;339:114-115.

7 Tuttleman JS, Pourcel C, Summers J: Formation of the pool of covalently closed circular viral dna in hepadnavirus-infected cells. Cell 1986;47:451-460.

8 Sureau C, Romet-Lemonne JL, Mullins JI, Essex M: Production of hepatitis b virus by a differentiated human hepatoma cell line after transfection with cloned circular hbv dna. Cell 1986;47:37-47.

9 Günther S, Li BC, Miska S, Krüger DH, Meisel H, Will H: A novel method for efficient amplification of whole hepatitis b virus genomes permits rapid functional analysis and reveals deletion mutants in immunosuppressed patients. J Virol 1995;69:5437-5444.

10 Summers J, Mason WS: Replication of the genome of a hepatitis b--like virus by reverse transcription of an rna intermediate. Cell 1982;29:403-415.

11 Chang CM, Jeng KS, Hu CP, Lo SJ, Su TS, Ting LP, Chou CK, Han SH, Pfaff E, Salfeld J: Production of hepatitis b virus in vitro by transient expression of cloned hbv dna in a hepatoma cell line. EMBO J 1987;6:675-680.

12 Delaney WE, Isom HC: Hepatitis b virus replication in human hepg2 cells mediated by hepatitis b virus recombinant baculovirus. Hepatology 1998;28:1134-1146.

13 Mercer DF, Schiller DE, Elliott JF, Douglas DN, Hao C, Rinfret A, Addison WR, Fischer KP, Churchill TA, Lakey JR, Tyrrell DL, Kneteman NM: Hepatitis c virus replication in mice with chimeric human livers. Nat Med 2001;7:927-933.

14 Chayama K, Hayes CN, Hiraga N, Abe H, Tsuge M, Imamura M: Animal model for study of human hepatitis viruses. J Gastroenterol Hepatol 2011;26:13-18.

15 Meuleman P, Libbrecht L, De Vos R, de Hemptinne B, Gevaert K, Vandekerckhove J, Roskams T, Leroux-Roels G: Morphological and biochemical characterization of a human liver in a upa-scid mouse chimera. Hepatology 2005;41:847-856.

16 Sainz B, Barretto N, Martin DN, Hiraga N, Imamura M, Hussain S, Marsh KA, Yu X, Chayama K, Alrefai WA, Uprichard SL: Identification of the niemann-pick c1-like 1 cholesterol absorption receptor as a new hepatitis c virus entry factor. Nat Med 2012;18:281-285.

17 Tsuge M, Takahashi S, Hiraga N, Fujimoto Y, Zhang Y, Mitsui F, Abe H, Kawaoka T, Imamura M, Ochi H, Hayes CN, Chayama K: Effects of hepatitis b virus infection on the interferon response in immunodeficient human hepatocyte chimeric mice. J Infect Dis 2011;204:224-228.

18 Tsuge M, Hiraga N, Takaishi H, Noguchi C, Oga H, Imamura M, Takahashi S, Iwao E, Fujimoto Y, Ochi H, Chayama K, Tateno C, Yoshizato K: Infection of human hepatocyte chimeric mouse with genetically engineered hepatitis b virus. Hepatology 2005;42:1046-1054.

19 Gripon P, Rumin S, Urban S, Le Seyec J, Glaise D, Cannie I, Guyomard C, Lucas J, Trepo C, Guguen-Guillouzo C: Infection of a human hepatoma cell line by hepatitis b virus. Proc Natl Acad Sci U S A 2002;99:15655-15660.

20 Yamada T, Jung J, Seno M, Kondo A, Ueda M, Tanizawa K, Kuroda S: Electroporation and use of hepatitis b virus envelope l proteins as bionanocapsules. Cold Spring Harb Protoc 2012;2012:702-705.

21 Yamada T, Iwasaki Y, Tada H, Iwabuki H, Chuah MK, VandenDriessche T, Fukuda H, Kondo A, Ueda M, Seno M, Tanizawa K, Kuroda S: Nanoparticles for the delivery of genes and drugs to human hepatocytes. Nat Biotechnol 2003;21:885-890.

22 Bartel DP: Micrornas: Target recognition and regulatory functions. Cell 2009;136:215-233.

23 Kishikawa T, Otsuka M, Yoshikawa T, Ohno M, Takata A, Shibata C, Kondo Y, Akanuma M, Yoshida H, Koike K: Regulation of the expression of the liver cancer susceptibility gene mica by micrornas. Sci Rep 2013;3:2739.

24 Kumar V, Kato N, Urabe Y, Takahashi A, Muroyama R, Hosono N, Otsuka M, Tateishi R, Omata M, Nakagawa H, Koike K, Kamatani N, Kubo M, Nakamura Y, Matsuda K: Genome-wide association study identifies a susceptibility locus for hcv-induced hepatocellular carcinoma. Nat Genet 2011;43:455-458.

25 Kumar V, Yi Lo PH, Sawai H, Kato N, Takahashi A, Deng Z, Urabe Y, Mbarek H, Tokunaga K, Tanaka Y, Sugiyama M, Mizokami M, Muroyama R, Tateishi R, Omata M, Koike K, Tanikawa C, Kamatani N, Kubo M, Nakamura Y, Matsuda K: Soluble mica and a mica variation as possible prognostic biomarkers for hbv-induced hepatocellular carcinoma. PLoS One 2012;7:e44743.

26 Pan XB, Ma H, Jin Q, Wei L: Characterization of microrna expression profiles associated with hepatitis b virus replication and clearance in vivo and in vitro. J Gastroenterol Hepatol 2012;27:805-812.

27 Niu Y, Wu Z, Shen Q, Song J, Luo Q, You H, Shi G, Qin W: Hepatitis b virus x protein co-activates pregnane x receptor to induce the cytochrome p450 3a4 enzyme, a potential implication in hepatocarcinogenesis. Dig Liver Dis 2013;45:1041-1048.

28 Mills JB, Rose KA, Sadagopan N, Sahi J, de Morais SM: Induction of drug metabolism enzymes and mdr1 using a novel human hepatocyte cell line. J Pharmacol Exp Ther 2004;309:303-309.

29 Stern-Ginossar N, Gur C, Biton M, Horwitz E, Elboim M, Stanietsky N, Mandelboim M, Mandelboim O: Human micrornas regulate stress-induced immune responses mediated by the receptor nkg2d. Nat Immunol 2008;9:1065-1073.

30 Yamada T, Iwabuki H, Kanno T, Tanaka H, Kawai T, Fukuda H, Kondo A, Seno M, Tanizawa K, Kuroda S: Physicochemical and immunological characterization of hepatitis b virus envelope particles exclusively consisting of the entire l (pre-s1 + pre-s2 + s) protein. Vaccine 2001;19:3154-3163.

31 Jung J, Matsuzaki T, Tatematsu K, Okajima T, Tanizawa K, Kuroda S: Bio-nanocapsule conjugated with liposomes for in vivo pinpoint delivery of various materials. J Control Release 2008;126:255-264.

32 Guo H, Ingolia NT, Weissman JS, Bartel DP: Mammalian micrornas predominantly act to decrease target mrna levels. Nature 2010;466:835-840.

33 Meister G: Mirnas get an early start on translational silencing. Cell 2007;131:25-28.

34 Chitadze G, Lettau M, Bhat J, Wesch D, Steinle A, Fürst D, Mytilineos J, Kalthoff H, Janssen O, Oberg HH, Kabelitz D: Shedding of endogenous mhc class i-related chain molecules a and b from different human tumor entities: Heterogeneous involvement of the "A disintegrin and metalloproteases" 10 and 17. Int J Cancer 2013;133:1557-1566.

35 Jung J, Iijima M, Yoshimoto N, Sasaki M, Niimi T, Tatematsu K, Jeong SY, Choi EK, Tanizawa K, Kuroda S: Efficient and rapid purification of drug- and gene-carrying bio-nanocapsules, hepatitis b virus surface antigen l particles, from saccharomyces cerevisiae. Protein Expr Purif 2011;78:149-155.

36 Honda M, Kaneko S, Kawai H, Shirota Y, Kobayashi K: Differential gene expression between chronic hepatitis b and c hepatic lesion. Gastroenterology 2001;120:955-966.

37 Otsuka M, Aizaki H, Kato N, Suzuki T, Miyamura T, Omata M, Seki N: Differential cellular gene expression induced by hepatitis b and c viruses. Biochem Biophys Res Commun 2003;300:443-447.

38 Wang X, Yuan ZH, Zheng LJ, Yu F, Xiong W, Liu JX, Hu GX, Li Y: Gene expression profiles in an hepatitis b virus transfected hepatoblastoma cell line and differentially regulated gene expression by interferon-alpha. World J Gastroenterol 2004;10:1740-1745.

39 Dandri M, Locarnini S: New insight in the pathobiology of hepatitis b virus infection. Gut 2012;61 Suppl 1:i6-17.

40 Wang H, Ryu WS: Hepatitis b virus polymerase blocks pattern recognition receptor signaling via interaction with ddx3: Implications for immune evasion. PLoS Pathog 2010;6:e1000986.

41 Fisicaro P, Valdatta C, Boni C, Massari M, Mori C, Zerbini A, Orlandini A, Sacchelli L, Missale G, Ferrari C: Early kinetics of innate and adaptive immune responses during hepatitis b virus infection. Gut 2009;58:974-982.

42 Banaudha K, Kaliszewski M, Korolnek T, Florea L, Yeung ML, Jeang KT, Kumar A: Microrna silencing of tumor suppressor dlc-1 promotes efficient hepatitis c virus replication in primary human hepatocytes. Hepatology 2011;53:53-61.

43 Yamasaki C, Tateno C, Aratani A, Ohnishi C, Katayama S, Kohashi T, Hino H, Marusawa H, Asahara T, Yoshizato K: Growth and differentiation of colony-forming human hepatocytes in vitro. J Hepatol 2006;44:749-757.

44 Takata A, Otsuka M, Yoshikawa T, Kishikawa T, Hikiba Y, Obi S, Goto T, Kang YJ, Maeda S, Yoshida H, Omata M, Asahara H, Koike K: Microrna-140 acts as a liver tumor suppressor by controlling nf-κb activity by directly targeting dna methyltransferase 1 (dnmt1) expression. Hepatology 2013;57:162-170.

45 Kojima K, Takata A, Vadnais C, Otsuka M, Yoshikawa T, Akanuma M, Kondo Y, Kang YJ, Kishikawa T, Kato N, Xie Z, Zhang WJ, Yoshida H, Omata M, Nepveu A, Koike K: Microrna122 is a key regulator of α-fetoprotein expression and influences the aggressiveness of hepatocellular carcinoma. Nat Commun 2011;2:338.

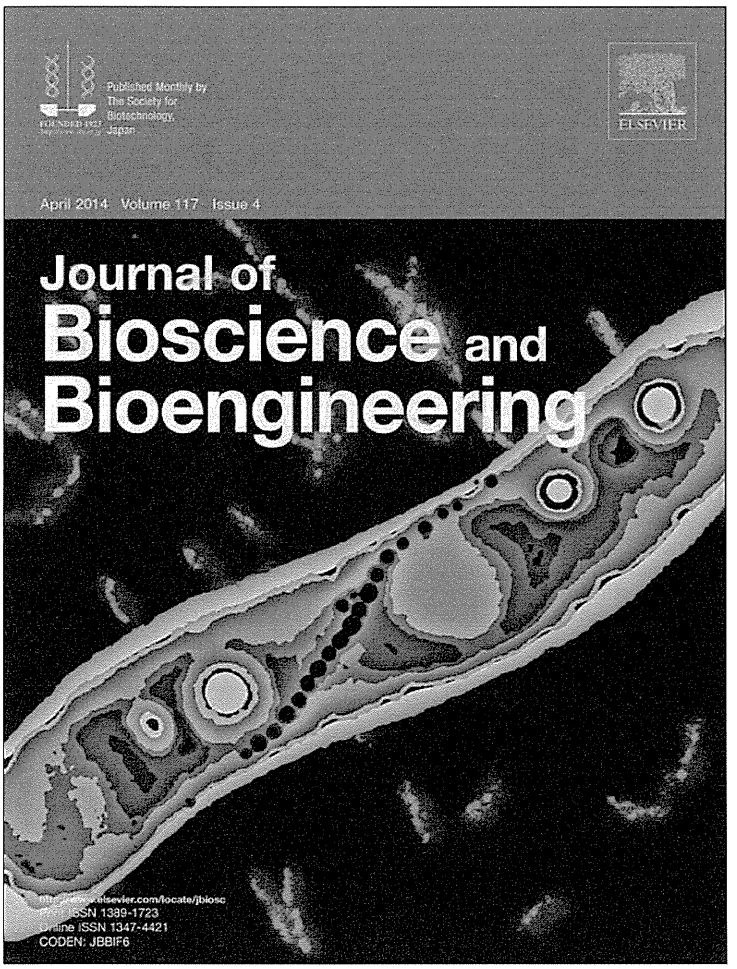

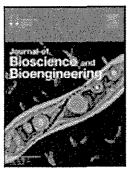

Journal of Bioscience and Bioengineering
VOL. 117 No. 4, 394–400, 2014

ELSEVIER

www.elsevier.com/locate/jbiosc

REVIEW

Single-cell-based breeding: Rational strategy for the establishment of cell lines from a single cell with the most favorable properties

Nobuo Yoshimoto and Shun'ichi Kuroda*

Graduate School of Bioagricultural Sciences, Nagoya University, Furo-cho, Chikusa, Nagoya, Aichi 464-8601, Japan

Received 11 July 2013; accepted 28 September 2013
Available online 9 November 2013

For efficient biomolecule production (e.g., antibodies, recombinant proteins), mammalian cells with high expression rates should be selected from cell libraries, propagated while maintaining a homogenous expression rate, and subsequently stabilized at their high expression rate. Clusters of isogenic cells (i.e., colonies) have been used for these processes. However, cellular heterogeneity makes it difficult to obtain cell lines with the highest expression rates by using single-colony-based breeding. Furthermore, even among the single cells in an isogenic cell population, the desired cell properties fluctuate stochastically during long-term culture. Therefore, although the molecular mechanisms underlying stochastic fluctuation are poorly understood, it is necessary to establish excellent cell lines in order to breed single cells to have higher expression, higher stability, and higher homogeneity while suppressing stochastic fluctuation (i.e., single-cell-based breeding). In this review, we describe various methods for manipulating single cells and facilitating single-cell analysis in order to better understand stochastic fluctuation. We demonstrated that single-cell-based breeding is practical and promising by using a high-throughput automated system to analyze and manipulate single cells.

[**Key words:** Automated single cell analysis and isolation system; Cellular heterogeneity; Biomolecule production; Stem cells; Hybridomas; Chinese hamster ovary cells]

Mammalian cells have been utilized for long time as a resource in the manufacture of biomolecules and biopharmaceuticals. Hybridomas and Chinese hamster ovary (CHO) cells are the most common cells used in this field (1,2). For efficient production of biomolecules using these cells, it is essential to select cells from cell libraries based on their high expression rate, propagate the cells while maintaining a homogeneous expression rate, and stabilize the high expression rate for long-term culture. Cell screenings for conventional methods of addressing these issues (mass production, cellular homogeneity, and cellular stability) have so far only been executed at the colony level (i.e., single-colony-based breeding; Fig. 1A). Candidate colonies are initially isolated using selection markers [e.g., drug resistance (3–5), auxotrophy (6,7), reporter gene expression (8–10)], subjected to limiting dilution (11), and then evaluated by immunoassays and/or functional assays to identify the single colonies with the highest expression. Recently, the detection and retrieval of those colonies with the most favorable properties have been performed automatically using the robotic system ClonePix FL (12). This system uses fluorescence-linked immunosorbent assay (FIA) to detect colonies that have the highest expression rates in groups of candidate colonies that are grown in a semi-solid medium. The system then uses a metal capillary to retrieve the colonies. Cell lines are established from the selected colonies by propagation over several passages and further evaluation of the stability of the higher rate of expression.

TWO MAJOR PROBLEMS OF CONVENTIONAL CELL BREEDING

After hybridomas established by the conventional ways are grown by fed-batch culture for more than 80 days, their expression decreased in a culture time-dependent manner (13). In addition, when isogenic IgG-producing CHO cells were separated into two groups (higher and lower IgG production) by fluorescence-activated cell sorter (FACS), the expression levels of both groups converged to that of parental cells after long-term culture (10). These spontaneous changes are considered to be due to the cellular heterogeneity in a selected single colony or stochastic fluctuation that occurs in each cell during long-term culture. Moreover, when single cells from isogenic hybridomas grow into single colonies of more than 4 cells, each colony has distinct levels of antibody expression because of stochastic fluctuation during the early phase of cell growth (14). Therefore, for effective establishment of cell lines, it is crucial to isolate single cells that have the highest expression rate as quickly as possible, and then propagate them homogeneously while minimizing the stochastic fluctuation (i.e., single-cell-based breeding; Fig. 1B). However, single cells cannot be manipulated in a high-throughput manner using conventional techniques. This makes it difficult to minimize cellular heterogeneity and determine the

* Corresponding author. Tel./fax: +81 52 789 5227.
E-mail address: skuroda@agr.nagoya-u.ac.jp (S. Kuroda).

1389-1723/$ – see front matter
http://dx.doi.org/10.1016/j.jbiosc.2013.09.016

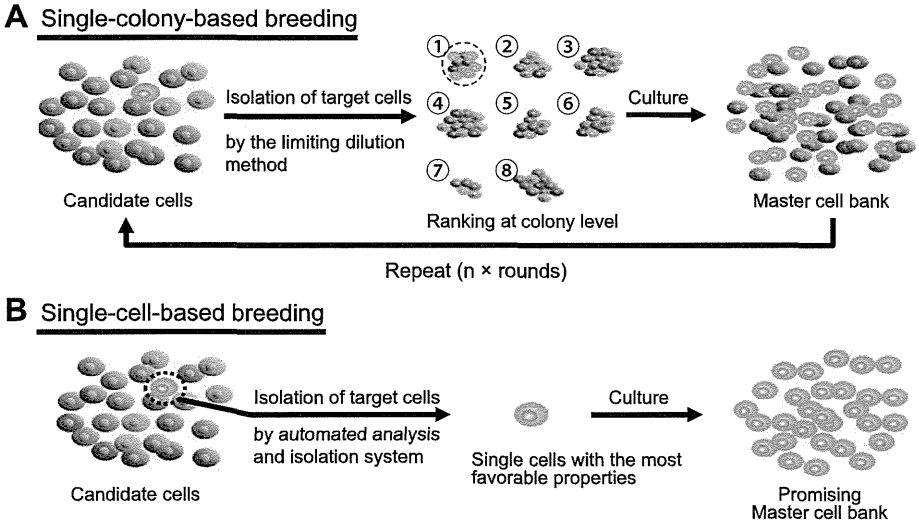

FIG. 1. Comparison of single-colony-based breeding (conventional) method with single-cell-based breeding (new) method. (A) Single-colony-based breeding. Candidate cells were divided into single cells by the limiting dilution method, and allowed to form colonies. Each colony was ranked based on the degree of favorable properties (light green cell showed the most favorable properties). Numbers in circles indicate the rank order of each colony. Top-ranked colony was further propagated to establish master cell bank, which was still contaminated with cells with non-favorable properties. The breeding process should be repeated *n* times to maximize the abundance of cells with favorable properties. The process is time-consuming and laborious. (B) Single-cell-based breeding. By using an automated single cell analysis and isolation system, cell showing the most favorable properties was isolated as a single colony. The cell was further propagated to establish master cell bank, which was completely devoid of the contamination of cells with non-favorable properties. Theoretically, it is not necessary to repeat the breeding process. (For interpretation of the references to color in this figure legend, the reader is referred to the web version of this article.)

molecular mechanisms that underlie stochastic fluctuation in specific single cells. On the other hand, substantial numbers of mammalian cell lines that were created by single-colony-based breeding for industrial production of biomolecules have been incidentally found to possess excellent mass productivity, cellular homogeneity, and cellular stability. This strongly suggests that the stochastic fluctuation was successfully suppressed in spite of the lack of precise knowledge about its mechanism. An automated system for manipulating single cells in a high-throughput manner that could identify single cells with the most favorable properties from huge number of candidate cells and isolate single cells of interest automatically would facilitate the refinement of cell breeding. This innovative approach would solve the problem of cellular heterogeneity, lead to the deciphering of the mechanisms of individual cell stochastic fluctuation, and facilitate the effective establishment of biomolecule-producing cells with high expression, homogeneity, and stability.

Here, we will provide an overview of the current techniques for single-cell analysis and isolation, and introduce an automated single-cell analysis and isolation system that we developed for single-cell-based breeding. We will also describe how to refine cell breeding using this system, and discuss the potential of this rational and reliable methodology for cell-based research and industry.

CURRENT TECHNIQUES FOR IDENTIFYING SINGLE CELLS WITH THE HIGHEST SECRETION RATE

To select single cells that secrete relatively large amounts of biomolecules, candidate cells in a cell library were often fluorescently labeled according to their secretion rates, and then subjected to fluorescent measurement, and single-cell isolation. This process requires nascent biomolecules to be retained within cell bodies by treating them with brefeldin A and labeling them with fluorophores, which severely affects cell viability and prevents the isolated cells from producing biomolecules. To accomplish single-cell-based breeding in a non-destructive, high-yield, and high-throughput manner, a reporter gene that encodes a fluorescent protein is introduced into the biomolecule gene using an internal ribosome entry site (IRES) (8). This allows the fluorescent measurement of the expression rate of each cell (Fig. 2A). However, this bicistronic reporter assay requires additional genetic modification and directly evaluates the synthesis rate of biomolecules, not their secretion rate. Gel microdrop assays have been used to measure secretion. For this assay, candidate cells are grown in a solid-medium containing biotinylated agarose, streptavidin, and biotinylated capture antibody. The cells are then formulated into gel microdrops, and placed in contact with fluorescence-labeled detection antibodies. The secreted biomolecules of each cell are then immobilized in the agarose matrix of the gel microdrop and form fluorescence-labeled immunocomplexes (Fig. 2B) (15). This method can be adapted to high-throughput isolation of efficient biomolecule-producing cells in a secretion-dependent manner, but both low encapsulation efficiency of cells (<15% of gel microdrops) and the physical stress caused by the solid medium remain to be addressed. Moreover, to avoid the encapsulation of cells into gel microdrops, the cell surface is initially coated with semi-solid medium, chemically labeled with biotin, and then mixed with neutravidin and biotinylated capture antibody. Secreted biomolecules immobilized as an immunocomplex in the vicinity of cells are detected by fluorescence-labeled detection antibody. This assay is known as the matrix-based secretion assay (Fig. 2C) (16). Although this assay is more efficient than the gel microdrop assay, the cells still suffer from chemical stress caused by direct biotinylation. More recently, a cell-surface fluorescence-linked immunosorbent assay (CS-FIA) was developed to measure the amount of nascent biomolecules secreted from single cells in a non-destructive manner (17). After the surface of candidate cells is modified with non-toxic lipid-labeled capture antibodies, nascent secreted antibodies are captured on the cell surface and subsequently detected with fluorescence-labeled detection antibodies (Fig. 2D). This method can be used to measure the amount of captured antibodies with extremely high sensitivity (from 6.25 fg/cell to 6.40 pg/cell). CS-FIA is a promising and reliable non-destructive and high-throughput method for identifying the individual cells that most efficiently secrete biomolecules.

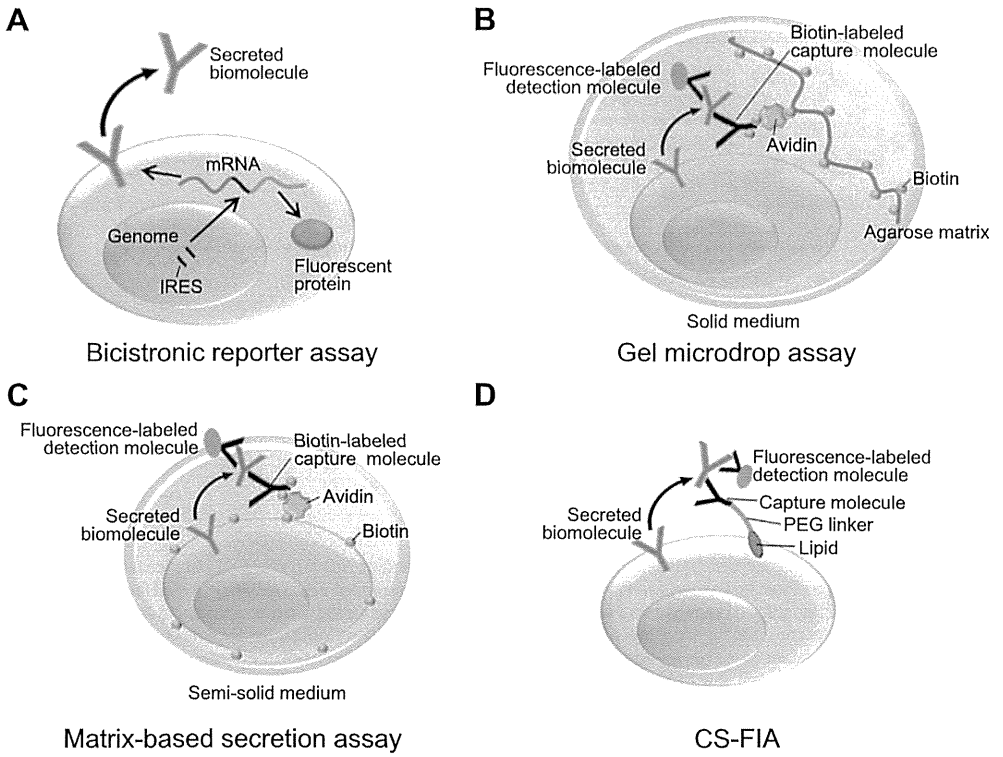

FIG. 2. Fluorescence-labeling techniques for single cells in a biomolecule secretion level-dependent manner. (A) Bicistronic reporter assay. A fluorescent protein gene was placed under the biomolecule gene of expression cassette by using internal ribosome entry site (IRES). This assay allows real-time measuring the transcription level of biomolecule gene in each cell, not always reflecting the secretion level. (B) Gel microdrop assay. Each cell was encapsulated in a solid medium microdrop containing biotinylated agarose, avidin, and biotin-labeled capture molecule. Biomolecules secreted from each cell were immobilized on the agarose matrix, and then sandwiched with fluorescence-labeled detection molecules. Fluorescence intensity of each cell increases in proportion to the secretion rate of biomolecules from each cell. (C) Matrix-based secretion assay. Surface of each cell was chemically labeled with biotin, and then each cell was encapsulated in a semi-solid medium containing avidin and biotin-labeled capture molecules. Secreted biomolecules were immobilized with biotin-labeled capture molecules at cell surface, and then sandwiched with fluorescence-labeled detection molecules. Fluorescence intensity of each cell increases in proportion to the secretion rate of biomolecules from each cell. (D) Cell-surface fluorescence-linked immunosorbent assay (CS-FIA). Each cell was incubated with lipid-PEG (polyethylene glycol)-labeled capture molecules for displaying the moiety of capture molecules onto cell surface spontaneously. Secreted biomolecules were immobilized with capture molecules at cell surface, and then sandwiched with fluorescence-labeled detection molecules. Fluorescence intensity of each cell increases in proportion to the secretion rate of biomolecules from each cell.

CONVENTIONAL TECHNIQUES FOR SINGLE-CELL ANALYSIS AND ISOLATION

The limiting dilution method has long been used to generate single colonies from single cells in order to isolate single cells with favorable properties (e.g., the highest synthesis and secretion rate of biomolecules). Candidate cells are serially diluted in multi-well plates so that each well contains approximately 1 cell. The cells then undergo long-term culture (3–7 days) for colony formation. Either supernatant or cell lysate of each colony is then subjected to enzyme-linked immunosorbent assay (ELISA) or to a functional assay in order to rank the colonies by according to the degree of favorable properties (e.g., productivity of biomolecules) (see nos. 1–8 with circle in Fig. 1A). Because the cells within a colonies are often heterogeneous, limiting dilution should be repeated until a colony with low cellular heterogeneity is obtained that also has the most favorable properties (14,18). The limiting dilution method is laborious, time-consuming, and unsuitable for high-throughput screening.

FACS, which uses fluorescence as an indicator for the most favorable cell properties, has been widely used for a high-throughput single-cell analysis and isolation in biological and biomedical fields (1). In this method, cells in sheath solution are introduced at high flow velocity ($\sim 10^4$ cells/sec) in a high-pressure flow path ($\sim$70 psi) to align them in a laminar flow formation. Target cells are identified using an optical system based on their fluorescent intensities and are then sorted into reservoir wells using high voltage ($\sim 6 \times 10^3$ V). At least 10^5 cells at a density of 10^5–10^6 cells/ml (19,20) are necessary for FACS analysis. Positive cells should make up more than 0.1% of the candidate cells (21), which is the threshold for discriminating them from background cells spectrophotometrically. Before cell sorting, a portion of the cell sample must be discarded in order to optimize the measurement conditions. Additionally, single cells isolated by FACS generally suffer from chemical stress derived from the sheath solution, mechanical stress from laminar flow formation, and electrical stress from sorting (22,23). These issues render FACS unsuitable for rare cells (less than 10^5 cells), diluted cells (less than 10^5 cells/ml), samples containing less than 0.1% positive cells, and vulnerable cells.

As an alternative to FACS, on-chip flow cytometers have been developed that use microfluidics (24–26). Single cells in a culture medium are flowed at a moderate flow velocity ($\sim 5 \times 10^2$ cells/sec) under atmospheric pressure through a microchannel that is $\sim$80 μm in diameter. The cells of interest are identified by their fluorescent intensities, and are sorted to reservoir wells by weak voltage ($\sim$6 V). Using this method, the processing rate can be increased by increasing the number of microchannels in parallel. This system is suitable for rare cells and vulnerable cells. However, probably due to the failure of cells to align in the microchannels, this system is only able to detect 70% of positive cells in samples (27).

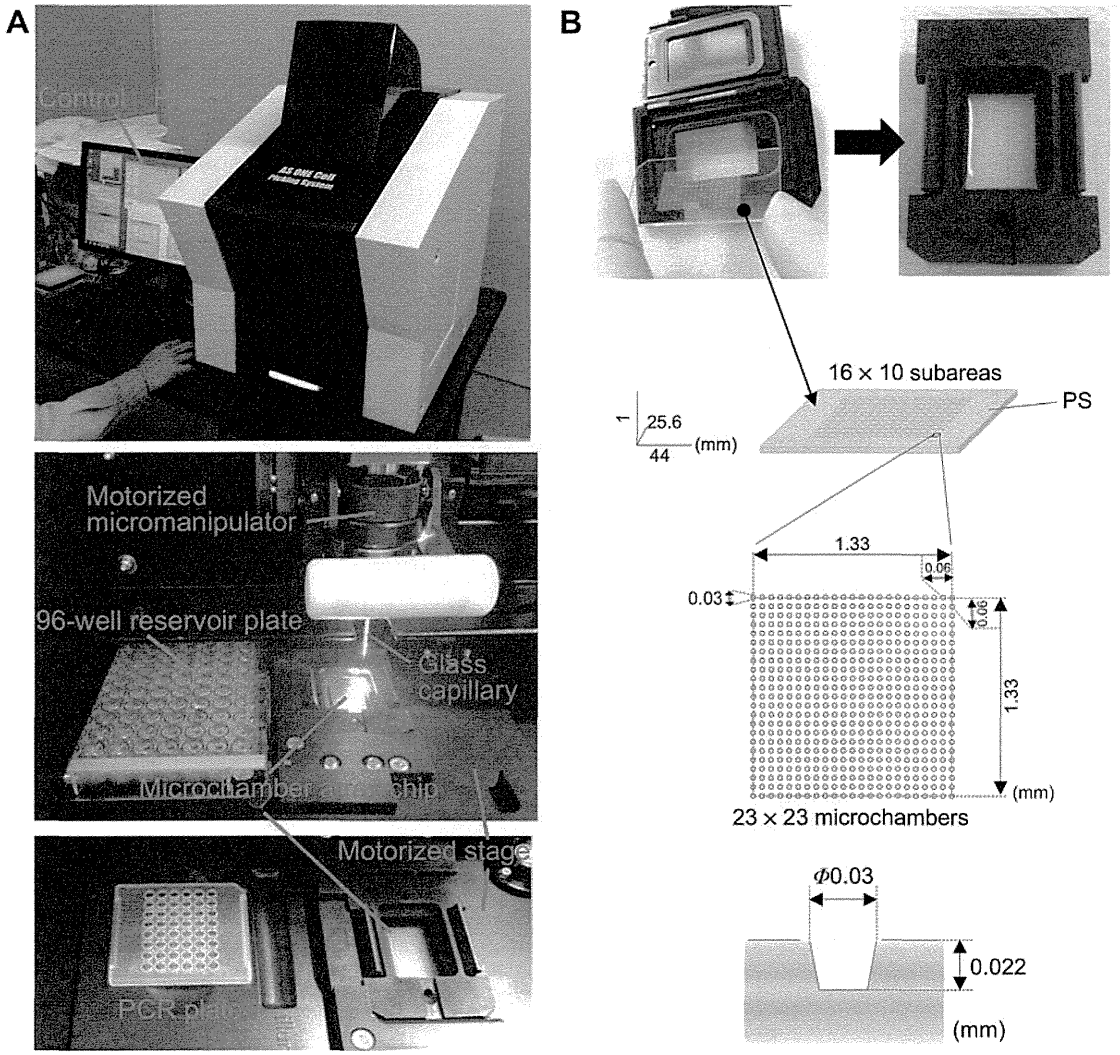

FIG. 3. Automated single-cell analysis and isolation system. (A) Overview of the robot (top). The robot consists of a motorized micromanipulator equipped with a glass capillary, a motorized stage, a reservoir plate (e.g., 6-, 12-, 24-, 48-, 96-, or 384-well format; 48- or 96-well PCR plate), and a microchamber array chip (middle and bottom). (B) Microchamber array chip. A microchamber array chip (1 × 25.6 × 44 mm) made of polystyrene (PS) consists of 16 × 10 subareas, each of which contains 23 × 23 microchambers (30 μm in diameter, 22 μm in depth).

CELL ARRAY SYSTEMS

In cell array systems, each cell is accommodated into a microchamber (10–30 μm in diameter, approximately 2×10^5 microchambers/chip) made of various polymers, such as, polystyrene, polymethylmethacrylate, polydimethylsiloxane, or silicon substrates (21,28,29). These cell arrays are subjected to large-scale analysis of single cells under mild conditions (atmospheric pressure, culture medium). The cells of interest can be detected at the single-cell level with a high signal to noise ratio, which excludes contamination by pseudo-positive cells in the same microchamber. However, because this method involves manual cell isolation is using a micromanipulator, a semi-automated colony isolation system, CellCelector, has been optimized as a single-cell isolation system (30). In this system, one or a few antibody-secreting cells are accommodated into cuboid microchambers (50 μm wide × 50 μm height × 50 μm depths) and covered with a glass slip coated with capturing molecules (anti-IgG antibodies). After removing the glass slip, the secreted antibodies captured on the slip are visualized with fluorescence-labeled secondary antibodies or specific antigens for identifying the cells that secrete antigen-specific antibodies. After matching the positions of the glass slip with those of microchambers, the cells of interest are automatically retrieved from the respective microchambers using a glass capillary. A similar automated single-cell isolation system, Cellporter, has been recently developed (31). When cells in microchambers (10 μm in diameter, 15 μm depths) were stimulated by oxidative or acidic stress, the responsive cells are manually identified by an independent fluorometric system and then each cell is automatically retrieved using a metal capillary. Both CellCelector and Cellporter systems facilitate the isolation of single cells from rare samples (less than 10^5 cells), diluted samples (less than 10^5 cells/ml), samples containing less than 0.1% positive cells, and vulnerable samples. However, both systems still require an additional device for identifying the cells of interest, which significantly reduces their processing capabilities. Therefore, the development of a fully automated system for single-cell analysis and isolation has been eagerly awaited.

AUTOMATED SINGLE-CELL ANALYSIS AND ISOLATION SYSTEM

We recently developed a stand-alone automated system for high-throughput single-cell analysis and isolation (Fig. 3A) (32). This system consists of a motorized stage (for *xy* movements, <1-μm movement accuracy), a motorized micromanipulator (for *z* movement, <0.1-μm movement accuracy), a pencil pump, a glass

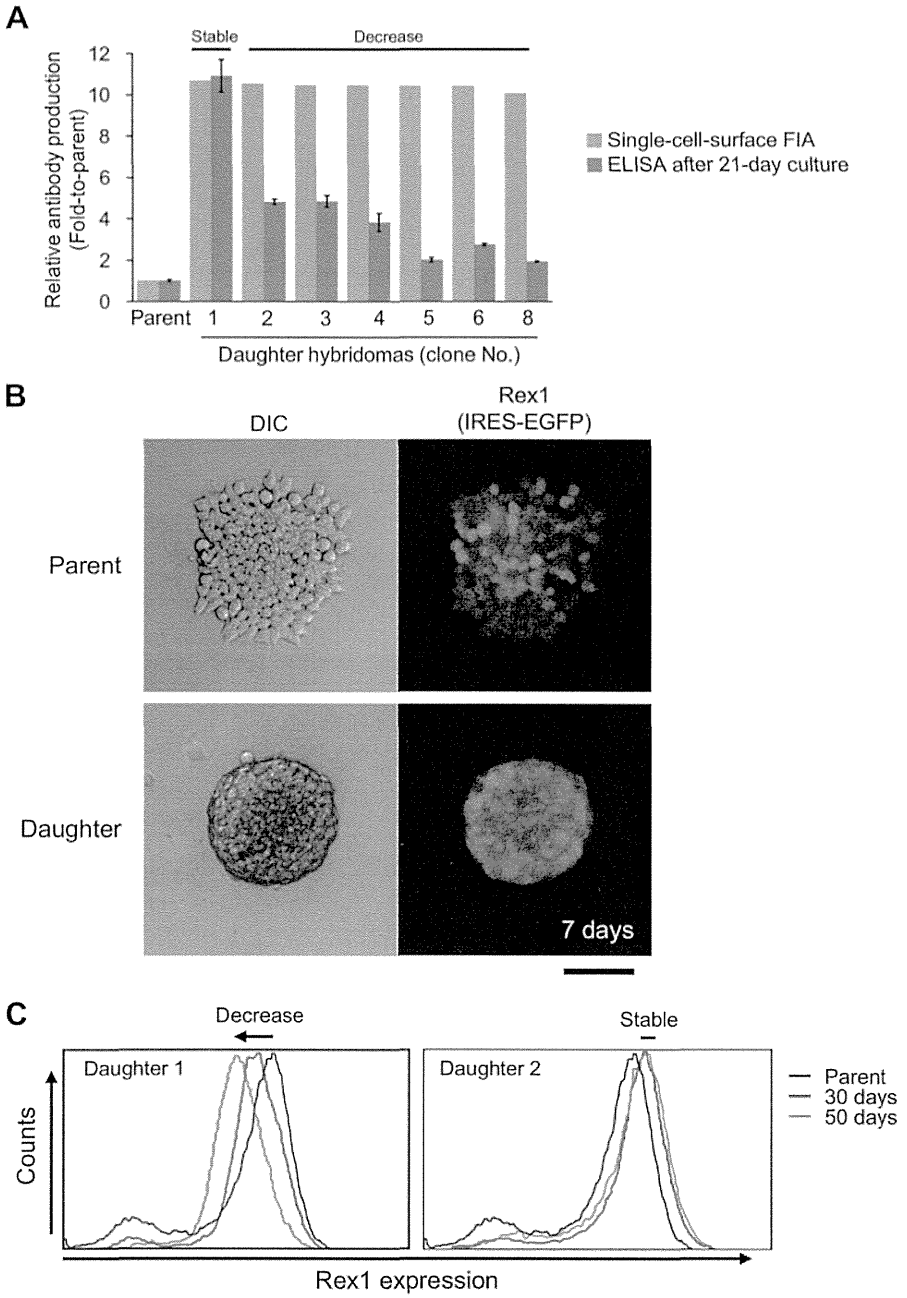

FIG. 4. Single-cell-based breeding of hybridomas and embryonic stem cells. (A) Fluctuation of antibody secretion rate of hybridomas after the propagation from single cells (21 days). Parent hybridomas (antibody secretion was optimized by single-colony-based breeding method) were subjected to CS-FIA (cyan bars), and then single hybridomas showing highest secretion rate (daughter hybridomas) were isolated by the automated single-cell analysis and isolation system. After these hybridomas were propagated for 21 days, culture media were analyzed by ELISA for the determination of secretion rate of antibodies (magenta bars). The antibody secretion rate of clone no. 1 was found stable during at least 21-day culture from single cell isolation, while those of other clones were found to be decreased. Error bars, $p < 0.05$, $n = 6$. (B) Colony formation of single ES cell showing highest expression of pluripotent marker *Rex1* gene. Mouse ES cells harboring *Rex1-IRES-EGFP* gene (parent cells) were subjected to the automated single-cell analysis and isolation system. Single cell showing highest *Rex1* expression (daughter cell) was automatically identified and subsequently isolated by the robot, and cultured to form colony for 7 days. Bars: 50 μm. (C) Fluctuation of pluripotent marker *Rex1* gene expression of daughter ES cells after the propagation from single cells (30 and 50 days). Parent ES cells (*Rex1* gene expression was optimized by single-colony-based breeding method) were subjected to the robot, and then two single cells showing highest *Rex1* gene expression (daughter cells nos. 1 and 2) were isolated by the robot. After the propagation for 30 and 50 days, parental, daughter no. 1, and daughter no. 2 cells were analyzed by FACS for the determination of *Rex1* gene expression. The *Rex1* gene expression of daughter no. 2 was found stable during at least 50-day culture from single cell isolation, while that of daughter no. 1 was found to be decreased.

capillary (40.5 μm inner diameter), fluorescence microscopy equipped with a CCD camera, a reservoir plate (6-, 12-, 24-, 48-, 96-, or 384-well format; 48- or 96-well PCR plate), a microchamber array chip (polystyrene, 30 μm in diameter, 22 μm in depth, 23 × 23 microchambers/subarea, 16 × 10 subareas/chip, 84,640 microchambers/chip; see also Fig. 3B), and a control computer. After fluorometrically scanning all cells in a cell array (excitation at 405 nm, 488 nm, and 633 nm; 7 s/subarea), a histogram of fluorescent intensity from each cell is generated that is used to rank cells in order of fluorescent intensity. Simultaneously, the system generates a list of addresses, fluorescent intensities, and images, including a transmission image of each cell. The cells of interest are identified automatically or manually based on their fluorescent intensities. Microchambers containing more than 2

cells are automatically excluded. Selected cells are promptly retrieved one-by-one using a glass capillary, and are transferred to assigned reservoir wells (10 s/cell). The retrieval of selected cells is confirmed by the elimination of fluorescence in each microchamber. Upon failure, the system automatically repeats the isolation process for the cell. The automated single-cell analysis and isolation system maximizes the usability of cell array systems. Moreover, as the parts that come in contact with samples (i.e., microchamber array chips, glass capillaries, reservoir plates) are essentially disposable, the system significantly reduces the risk of contamination and infection, and is therefore more applicable than conventional cell analysis and isolation systems to research conducted in accordance with good laboratory practices (GLP) and production performed under good manufacturing practices (GMP).

SINGLE-CELL-BASED BREEDING OF HYBRIDOMAS AND EMBRYONIC STEM CELLS

We used the automated single-cell analysis and isolation system to select 362 cells that exhibited higher fluorescence than parental hybridomas from $\sim 5.0 \times 10^4$ hybridomas that were established by conventional methods and subjected to CS-FIA (Fig. 2D). Eight cells with the highest level of fluorescence were isolated by the system, and were further propagated to about $\sim 5.0 \times 10^5$ cells over 2 weeks. Finally, after 21 days of culture, 7 hybridomas were found to secret higher amounts (up to 10-fold) of antibodies than parental hybridomas (Fig. 4A) (32). Hybridoma clone no. 1 was able maintain the high secretion rate without any decrease for at least 35 days. The combination of the automated single-cell analysis and isolation system with CS-FIA was thus demonstrated to be effective and practical for improvement of the productivity of biomolecules that are secreted from various cells.

To establish mouse embryonic stem cells (ESCs) with the highest pluripotency, parental ESCs were firstly modified to incorporate the *EGFP* (enhanced green fluorescent protein) gene under the *Rex1* gene (a pluripotent marker) using a bicistronic reporter system (Fig. 2A). About 1.0×10^5 cells of parental ESCs were subjected to the automated single-cell analysis and isolation system and 25 single cells showing higher fluorescence were isolated. These cells were subsequently cultured for 7 days to form colonies. About 64% (16/25) of daughter cells formed more spherical colonies and exhibited more uniform fluorescence than parental cells (Fig. 4B). Furthermore, after 50 days, some portions of daughter cells were retained stable and high expression of the *Rex1* gene, indicating that the stochastic fluctuation of pluripotency was successfully suppressed by single-cell-based breeding (Fig. 4C). Taken together, the automated single-cell analysis and isolation system may resolve cellular heterogeneity; one of the two major problems that occur during conventional single-colony based breeding (see above). However, it is an indispensable tool for solving the problem of stochastic fluctuation, fully establishing the single-cell-based breeding.

MANAGEMENT OF STOCHASTIC FLUCTUATION FOR SINGLE-CELL-BASED BREEDING

Even among isogenic cells, stochastic fluctuation is often found in epigenetic modification (33,34), protein expression (35–37), transcription (38,39), and cell-cycle progression (40). Single-cell omics analyses of isogenic cells have recently revealed that these stochastic fluctuations occur at the level of individual cells. When cellular heterogeneity is successfully excluded from cell breeding using our system, the established cell lines often have reduced productivity of biomolecules during long-term culture. This might be caused by the stochastic fluctuation that occurs in each cell. To establish single-cell-based breeding, it is necessary to decipher the molecular basis underlying stochastic fluctuation and to thereby identify the master regulators that govern this fluctuation. These postulated regulators could be found using global analyses (e.g., genomics, epigenomics, transcriptomics, proteomics, and metabolomics) of cells with relatively high expression, stability, and homogeneity and using isogenic cells as controls. The use of the regulators as a marker in an automated single-cell analysis and isolation system would significantly increase the likelihood of isolating those cells with relatively low stochastic fluctuation. Furthermore, stochastic fluctuation could be minimized by managing the expression level of the regulators. Indeed, through the single-cell-based breeding of ESCs, Nanog, a pluripotent marker, has been identified as one of the master regulators that can be managed to maintain high pluripotency by suppressing stochastic fluctuation (41).

CONCLUDING REMARKS

In order to obtain the efficient secretion of biomolecules, cell lines should be established that avoid both cellular heterogeneity at the colony level and stochastic fluctuation at the single-cell level. The combination of the automated single-cell analysis and isolation system with CS-FIA allowed us to obtain single cells that efficiently secrete biomolecules, thereby excluding the influence of cellular heterogeneity in the colonies bred from these cells. To establish single-cell-based breeding, global analysis of these cells would be an effective method for identifying master regulators that govern stochastic fluctuation.

ACKNOWLEDGMENTS

This study was supported in part by Adaptable & Seamless Technology Transfer Program through Target-driven R&D (A-STEP) by the Japan Science and Technology Agency (JST) (AS231Z04687F to N.Y., AS2311699F to S.K.), the Program for Promotion of Basic and Applied Researches for Innovations in Bio-oriented Industry (H22-7, BRAIN to S.K.), a Grant-in-Aid for Scientific Research (A) (25242043 to S.K.), the Health Labor Sciences Research Grant from the Ministry of Health Labor and Welfare (to S.K.), and the As One Corporation (to S.K.). We thank Ken-ichi Kimura and Xu Jie (Furukawa), Masato Fujihashi and Masaya Kurokawa (Starlite), and Masahiro Matsushita, Kenji Uemukai, and Tohru Kaneno (As One).

References

1. **Herzenberg, L. A. and de Rosa, S. C.:** Monoclonal antibodies and the FACS: complementary tools for immunobiology and medicine, Immunol. Today, **21**, 383–390 (2000).
2. **Hacker, D. L., de Jesus, M., and Wurm, F. M.:** 25 Years of recombinant proteins from reactor-grown cells – where do we go from here? Biotechnol. Adv., **27**, 1023–1027 (2009).
3. **Wagman, G. H., Testa, R. T., Marquez, J. A., and Weinstein, M. J.:** Antibiotic G-418, a new micromonospora-produced aminoglycoside with activity against protozoa and helminths: fermentation, isolation, and preliminary characterization, Antimicrob. Agents Chemother., **6**, 144–149 (1974).
4. **Southern, P. J. and Berg, P.:** Transformation of mammalian cells to antibiotic resistance with a bacterial gene under control of the SV40 early region promoter, J. Mol. Appl. Genet., **1**, 327–341 (1982).
5. **Blochlinger, K. and Diggelmann, H.:** Hygromycin B phosphotransferase as a selectable marker for DNA transfer experiments with higher eucaryotic cells, Mol. Cell. Biol., **4**, 2929–2931 (1984).
6. **Littlefield, J. W.:** Selection of hybrids from matings of fibroblasts in vitro and their presumed recombinants, Science, **145**, 709–710 (1964).
7. **Simonsen, C. C. and Levinson, A. D.:** Isolation and expression of an altered mouse dihydrofolate reductase cDNA, Proc. Natl. Acad. Sci. USA, **80**, 2495–2499 (1983).
8. **Gurtu, V., Yan, G., and Zhang, G.:** IRES bicistronic expression vectors for efficient creation of stable mammalian cell lines, Biochem. Biophys. Res. Commun., **229**, 295–298 (1996).

9. **Mancia, F., Patel, S. D., Rajala, M. W., Scherer, P. E., Nemes, A., Schieren, I., Hendrickson, W. A., and Shapiro, L.:** Optimization of protein production in mammalian cells with a coexpressed fluorescent marker, Structure, **12**, 1355–1360 (2004).
10. **Pilbrough, W., Munro, T. P., and Gray, P.:** Intraclonal protein expression heterogeneity in recombinant CHO cells, PLoS One, **4**, e8432 (2009).
11. **Lietzke, R. and Unsicker, K.:** A statistical approach to determine monoclonality after limiting cell plating of a hybridoma clone, J. Immunol. Methods, **76**, 223–228 (1985).
12. **Caron, A. W., Nicolas, C., Gaillet, B., Ba, I., Pinard, M., Garnier, A., Massie, B., and Gilbert, R.:** Fluorescent labeling in semi-solid medium for selection of mammalian cells secreting high-levels of recombinant proteins, BMC Biotechnol., **9**, 42 (2009).
13. **Frame, K. K. and Hu, W. S.:** The loss of antibody productivity in continuous culture of hybridoma cells, Biotechnol. Bioeng., **35**, 469–476 (1990).
14. **Gardner, J. S., Chiu, A. L., Maki, N. E., and Harris, J. F.:** A quantitative stability analysis of human monoclonal antibody production by heteromyeloma hybridomas, using an immunofluorescent technique, J. Immunol. Methods, **85**, 335–346 (1985).
15. **Akselband, Y., Moen, P. T., Jr., and McGrath, P.:** Isolation of rare isotype switch variants in hybridoma cell lines using an agarose gel microdrop-based protein secretion assay, Assay Drug Dev. Technol., **1**, 619–626 (2003).
16. **Manz, R., Assenmacher, M., Pflüger, E., Miltenyi, S., and Radbruch, A.:** Analysis and sorting of live cells according to secreted molecules, relocated to a cell-surface affinity matrix, Proc. Natl. Acad. Sci. USA, **92**, 1921–1925 (1995).
17. **Kida, A., Iijima, M., Niimi, T., Maturana, A. D., Yoshimoto, N., and Kuroda, S.:** Cell surface-fluorescence immunosorbent assay for real-time detection of hybridomas with efficient antibody secretion at the single-cell level, Anal. Chem., **85**, 1753–1759 (2013).
18. **Underwood, P. A. and Bean, P. A.:** Hazards of the limiting-dilution method of cloning hybridomas, J. Immunol. Methods, **107**, 119–128 (1988).
19. **Kurimoto, K., Yabuta, Y., Ohinata, Y., and Saitou, M.:** Global single-cell cDNA amplification to provide a template for representative high-density oligonucleotide microarray analysis, Nat. Protoc., **2**, 739–752 (2007).
20. **Ramsköld, D., Luo, S., Wang, Y. C., Li, R., Deng, Q., Faridani, O. R., Daniels, G. A., Khrebtukova, I., Loring, J. F., Laurent, L. C., Schroth, G. P., and Sandberg, R.:** Full-length mRNA-Seq from single-cell levels of RNA and individual circulating tumor cells, Nat. Biotechnol., **30**, 777–782 (2012).
21. **Yamamura, S., Kishi, H., Tokimitsu, Y., Kondo, S., Honda, R., Rao, S. R., Omori, M., Tamiya, E., and Muraguchi, A.:** Single-cell microarray for analyzing cellular response, Anal. Chem., **77**, 8050–8056 (2005).
22. **Ohgushi, M. and Sasai, Y.:** Lonely death dance of human pluripotent stem cells: ROCKing between metastable cell states, Trends Cell Biol., **21**, 274–282 (2011).
23. **Fong, C. Y., Peh, G. S., Gauthaman, K., and Bongso, A.:** Separation of SSEA-4 and TRA-1-60 labelled undifferentiated human embryonic stem cells from a heterogeneous cell population using magnetic-activated cell sorting (MACS) and fluorescence-activated cell sorting (FACS), Stem Cell Rev., **5**, 72–80 (2009).
24. **Takahashi, K., Hattori, A., Suzuki, I., Ichiki, T., and Yasuda, K.:** Non-destructive on-chip cell sorting system with real-time microscopic image processing, J. Nanobiotechnol., **2**, 5 (2004).
25. **Hayashi, M., Hattori, A., Kim, H., Terazono, H., Kaneko, T., and Yasuda, K.:** Fully automated on-chip imaging flow cytometry system with disposable contamination-free plastic re-cultivation chip, Int. J. Mol. Sci., **12**, 3618–3634 (2011).
26. **Fu, A. Y., Spence, C., Scherer, A., Arnold, F. H., and Quake, S. R.:** A microfabricated fluorescence-activated cell sorter, Nat. Biotechnol., **17**, 1109–1111 (1999).
27. **Takao, M. and Takeda, K.:** Enumeration, characterization, and collection of intact circulating tumor cells by cross contamination-free flow cytometry, Cytometry A, **79**, 107–117 (2011).
28. **Jin, A., Ozawa, T., Tajiri, K., Obata, T., Kondo, S., Kinoshita, K., Kadowaki, S., Takahashi, K., Sugiyama, T., Kishi, H., and other 1 author:** A rapid and efficient single-cell manipulation method for screening antigen-specific antibody-secreting cells from human peripheral blood, Nat. Med., **15**, 1088–1092 (2009).
29. **Figueroa, X. A., Cooksey, G. A., Votaw, S. V., Horowitz, L. F., and Folch, A.:** Large-scale investigation of the olfactory receptor space using a microfluidic microwell array, Lab Chip, **10**, 1120–1127 (2010).
30. **Choi, J. H., Ogunniyi, A. O., Du, M., Du, M., Kretschmann, M., Eberhardt, J., and Love, J. C.:** Development and optimization of a process for automated recovery of single cells identified by microengraving, Biotechnol. Prog., **26**, 888–895 (2010).
31. **Suzuki, M., Tanaka, H., and Iribe, Y.:** Detection and collection system of target single cell based on pH and oxygen sensing, J. Robot. Mechatron., **22**, 639–643 (2010).
32. **Yoshimoto, N., Kida, A., Jie, X., Kurokawa, M., Iijima, M., Niimi, T., Maturana, A. D., Nikaido, I., Ueda, H. R., Tatematsu, K., and other 4 authors:** An automated system for high-throughput single cell-based breeding, Sci. Rep., **3**, 1191 (2013).
33. **Obier, N. and Müller, A. M.:** Chromatin flow cytometry identifies changes in epigenetic cell states, Cells Tissues Organs, **191**, 167–174 (2010).
34. **Ben-David, U. and Benvenisty, N.:** The tumorigenicity of human embryonic and induced pluripotent stem cells, Nat. Rev. Cancer, **11**, 268–277 (2011).
35. **Irish, J. M., Kotecha, N., and Nolan, G. P.:** Mapping normal and cancer cell signalling networks: towards single-cell proteomics, Nat. Rev. Cancer, **6**, 146–155 (2006).
36. **Rosenfeld, N., Young, J. W., Alon, U., Swain, P. S., and Elowitz, M. B.:** Gene regulation at the single-cell level, Science, **307**, 1962–1965 (2005).
37. **Cai, L., Friedman, N., and Xie, X. S.:** Stochastic protein expression in individual cells at the single molecule level, Nature, **440**, 358–362 (2006).
38. **Aoi, T., Yae, K., Nakagawa, M., Ichisaka, T., Okita, K., Takahashi, K., Chiba, T., and Yamanaka, S.:** Generation of pluripotent stem cells from adult mouse liver and stomach cells, Science, **321**, 699–702 (2008).
39. **Ko, M. S.:** A stochastic model for gene induction, J. Theor. Biol., **153**, 181–194 (1991).
40. **Symeonidou, I. E., Taraviras, S., and Lygerou, Z.:** Control over DNA replication in time and space, FEBS Lett., **586**, 2803–2812 (2012).
41. **Macarthur, B. D., Sevilla, A., Lenz, M., Müller, F. J., Schuldt, B. M., Schuppert, A. A., Ridden, S. J., Stumpf, P. S., Fidalgo, M., Ma'ayan, A., and other 2 authors:** Nanog-dependent feedback loops regulate murine embryonic stem cell heterogeneity, Nat. Cell Biol., **14**, 1139–1147 (2012).

Amphipathic α-Helices in Apolipoproteins Are Crucial to the Formation of Infectious Hepatitis C Virus Particles

Takasuke Fukuhara[1☯], Masami Wada[1☯], Shota Nakamura[2], Chikako Ono[1], Mai Shiokawa[1], Satomi Yamamoto[1], Takashi Motomura[1], Toru Okamoto[1], Daisuke Okuzaki[3], Masahiro Yamamoto[4], Izumu Saito[5], Takaji Wakita[6], Kazuhiko Koike[7], Yoshiharu Matsuura[1]*

1 Department of Molecular Virology, Research Institute for Microbial Diseases, Osaka University, Osaka, Japan, **2** Department of Infection Metagenomics, Research Institute for Microbial Diseases, Osaka University, Osaka, Japan, **3** DNA-Chip Developmental Center for Infectious Diseases, Research Institute for Microbial Diseases, Osaka University, Osaka, Japan, **4** Department of Immunoparasitology, Research Institute for Microbial Diseases, Osaka University, Osaka, Japan, **5** Laboratory of Molecular Genetics, Institute of Medical Science, University of Tokyo, Tokyo, Japan, **6** Department of Virology II, National Institute of Infectious Diseases, Tokyo, Japan, **7** Department of Gastroenterology, Graduate School of Medicine, University of Tokyo, Tokyo, Japan

Abstract

Apolipoprotein B (ApoB) and ApoE have been shown to participate in the particle formation and the tissue tropism of hepatitis C virus (HCV), but their precise roles remain uncertain. Here we show that amphipathic α-helices in the apolipoproteins participate in the HCV particle formation by using zinc finger nucleases-mediated apolipoprotein B (ApoB) and/or ApoE gene knockout Huh7 cells. Although Huh7 cells deficient in either ApoB or ApoE gene exhibited slight reduction of particles formation, knockout of both ApoB and ApoE genes in Huh7 (DKO) cells severely impaired the formation of infectious HCV particles, suggesting that ApoB and ApoE have redundant roles in the formation of infectious HCV particles. cDNA microarray analyses revealed that ApoB and ApoE are dominantly expressed in Huh7 cells, in contrast to the high level expression of all of the exchangeable apolipoproteins, including ApoA1, ApoA2, ApoC1, ApoC2 and ApoC3 in human liver tissues. The exogenous expression of not only ApoE, but also other exchangeable apolipoproteins rescued the infectious particle formation of HCV in DKO cells. In addition, expression of these apolipoproteins facilitated the formation of infectious particles of genotype 1b and 3a chimeric viruses. Furthermore, expression of amphipathic α-helices in the exchangeable apolipoproteins facilitated the particle formation in DKO cells through an interaction with viral particles. These results suggest that amphipathic α-helices in the exchangeable apolipoproteins play crucial roles in the infectious particle formation of HCV and provide clues to the understanding of life cycle of HCV and the development of novel anti-HCV therapeutics targeting for viral assembly.

Citation: Fukuhara T, Wada M, Nakamura S, Ono C, Shiokawa M, et al. (2014) Amphipathic α-Helices in Apolipoproteins Are Crucial to the Formation of Infectious Hepatitis C Virus Particles. PLoS Pathog 10(12): e1004534. doi:10.1371/journal.ppat.1004534

Editor: Timothy L. Tellinghuisen, The Scripps Research Institute, United States of America

Received August 3, 2014; **Accepted** October 21, 2014; **Published** December 11, 2014

Data Availability: The authors confirm that all data underlying the findings are fully available without restriction. All relevant data are within the paper and its Supporting Information files except for the cDNA array data of GSE32886 which is available from GEO (Gene Expression Omnibus) under the accession number GSE32886.

Funding: This work was supported in part by grants-in-aid from the Japanese Ministry of Health, Labor, and Welfare (Research on Hepatitis), the Japanese Ministry of Education, Culture, Sports, Science, and Technology, the Naito Foundation, and the Takeda Science Foundation. The funders had no role in study design, data collection and analysis, decision to publish, or preparation of the manuscript.

Competing Interests: The authors have declared that no competing interests exist.

* Email: matsuura@biken.osaka-u.ac.jp

☯ These authors contributed equally to this work.

Introduction

More than 160 million individuals worldwide are infected with hepatitis C virus (HCV), and cirrhosis and hepatocellular carcinoma induced by HCV infection are life-threatening diseases [1]. Current standard therapy combining peg-interferon (IFN), ribavirin (RBV) and a protease inhibitor has achieved a sustained virological response (SVR) in over 80% of individuals infected with HCV genotype 1 [2]. In addition, many antiviral agents targeting non-structural proteins and host factors involved in HCV replication have been applied in clinical trials [3,4].

In vitro systems have been developed for the study of HCV infection and have revealed many details of the life cycle of HCV. By using pseudotype particles bearing HCV envelope proteins and RNA replicon systems, many host factors required for entry and RNA replication have been identified, respectively [5,6]. In addition, development of a robust *in vitro* propagation system of HCV based on the genotype 2a JFH1 strain (HCVcc) has gradually clarified the mechanism of assembly of HCV particles [7,8]. It has been shown that the interaction of NS2 protein with structural and non-structural proteins facilitates assembly of the viral capsid and formation of infectious particles at the connection site between the ER membrane and the surface of lipid droplets (LD) [9]. On the other hand, very low density lipoprotein (VLDL) associated proteins, including apolipoprotein B (ApoB), ApoE, and microsomal triglyceride transfer protein (MTTP), have been shown to play crucial roles in the formation of infectious HCV particles [10–12]. Generally, ApoA, ApoB, ApoC and ApoE bind the surface of lipoprotein through the interaction between amphipathic α-helices and ER-derived membrane [13,14]. This

Author Summary

In vitro systems have been developed for the study of hepatitis C virus (HCV) infection and have revealed many details of the life cycle of HCV. Apolipoprotein B (ApoB) and ApoE have been shown to play crucial roles in the particle formation of HCV, based on data obtained by siRNA-mediated gene knockdown and overexpression of the proteins. However, precise roles of the apolipoproteins in HCV assembly have not been elucidated yet. In this study, we show that infectious particle formation of HCV in Huh7 cells was severely impaired by the knockout of both ApoB and ApoE genes by artificial nucleases, and this reduction was cancelled by the expression of not only ApoE, but also other exchangeable apolipoproteins, including ApoA1, ApoA2, ApoC1, ApoC2 and ApoC3. In addition, expression of amphipathic α-helices in the exchangeable apolipoproteins restored the infectious particle formation in the double-knockout cells through an interaction with viral particles. These results provide clues to the understanding of life cycle of HCV and the development of novel antivirals to HCV.

binding of apolipoproteins enhances the stability and hydrophilicity of lipoprotein. However, the specific roles played by the apolipoproteins in HCV particle formation are controversial. Gastaminza et al. demonstrated that ApoB and MTTP are cellular factors essential for an efficient assembly of infectious HCV particles [10]. However, studies by other groups demonstrated that ApoE is a major determinant of the infectivity and particle formation of HCV, and the ApoE fraction is highly enriched with infectious particles [11]. In addition, Mancone et al. showed that ApoA1 is required for production of infectious particles of HCV [15]. However, the evidence of the involvement of apolipoproteins in HCV particle formation is dependent on knockdown data and exogenous expression of the apolipoproteins, and thus the precise mechanisms of participation of the apolipoproteins in HCV assembly have not been elucidated [10,11,16].

Recently, several novel genome editing techniques have been developed, including methods using zinc finger nucleases (ZFN), transcription activator like-effector nucleases (TALEN) and CRISPR/Cas9 systems [17–19]. DNA double strand breaks (DSBs) induced by these artificial nucleases can be repaired by error-prone non-homologous end joining (NHEJ), resulting in mutant mice or cell lines carrying deletions, insertions, or substitutions at the cut site. To clarify the detailed function of gene family with redundant functions, the generation of animals or cell lines carrying multiple mutated genes may be essential.

In this study, Huh7 cell lines deficient in both ApoB and ApoE genes were established by using ZFNs and revealed that ApoB and ApoE redundantly participate in the formation of infectious HCV particles. Interestingly, the expression of other exchangeable apolipoproteins, i.e., ApoA1, ApoA2, ApoC1, ApoC2 and ApoC3, facilitated HCV assembly in ApoB and ApoE double-knockout cells. In addition, the expression of amphipathic α-helices in the exchangeable apolipoproteins restored the production of infectious particles in the double-knockout cells through an interaction with viral particles.

Results

Several apolipoproteins participate in the production of infectious viral particles

First, we compared expression levels of apolipoproteins between hepatocyte and hepatic cancer cell lines including Huh7 and HepG2 cells (Fig. 1A and B). The web-based search engine NextBio (NextBio, Santa Clara, CA) revealed that ApoB, ApoH and the exchangeable apolipoproteins ApoA1, ApoA2, ApoC1, ApoC2, ApoC3, and ApoE are highly expressed in human liver tissues (Fig. 1A). On the other hand, the expressions of ApoA1, ApoC1, ApoC2, ApoC3 and ApoH in hepatic cancer cell lines were suppressed compared to those in hepatocytes (Fig. 1B). To examine the roles of apolipoproteins in the formation of infectious HCV particles, the effects of knockdown of ApoA2, ApoB and ApoE on the infectious particle production in the supernatants were determined in Huh7 cells by focus forming assay (Fig. 1C). The transfection of siRNAs targeting to ApoA2, ApoB and ApoE significantly suppressed the production of infectious HCV particles. This inhibitory effect is well consistent with the high level of expression of these apolipoproteins in the hepatic cancer cell lines, suggesting that the apolipoproteins involved in HCV assembly are dependent on the expression pattern in hepatic cancer cell lines, including Huh7 cells [20]. Therefore, we examined the effects of exogenous expression of the apolipoproteins highly expressed in the liver tissues on the infection of HCV in the stable ApoE-knockdown Huh7 cells (Fig. 1D). In contrast to the control-knockdown cells, expression of not only ApoE but also ApoA1, ApoA2, and ApoC1 rescued the infectious particle formation in the ApoE-knockdown cells (Fig. 1E), suggesting that various exchangeable apolipoproteins participate in the efficient production of infectious HCV particles.

ApoB and ApoE have a redundant role in HCV particle formation

To obtain more convincing data on the involvement of apolipoproteins in the production of infectious HCV particles, we established knockout (KO) Huh7 cells deficient in either ApoB (B-KO1 and B-KO2) or ApoE (E-KO1 and E-KO2) by using ZFN (Figure S1). Deficiencies of ApoB or ApoE expression in these cell lines were confirmed by ELISA and immunoblotting analyses (Figure S1). First, we examined the roles of ApoB and ApoE on the entry and RNA replication of HCV by using HCV pseudotype particles (HCVpp) and subgenomic replicon (SGR) of the JFH1 strain, respectively. The B-KO and E-KO cell lines exhibited no significant effect on the infectivity of HCVpp and the colony formation of SGR (Figure S2A and Figure S2B), suggesting that ApoB and ApoE are not involved in the entry and replication processes of HCV. To examine the role of ApoB and ApoE in the propagation of HCV, HCVcc was inoculated into parental, B-KO and E-KO cell lines at an MOI of 1, and intracellular viral RNA and infectious titers in the supernatants were determined (Figure S2C and Figure S2D). Although RNA replication and infectious particle formation in B-KO cells upon infection with HCV were comparable with those in parental Huh7 cells, E-KO cells exhibited slight reduction of particle formation, and the expression of ApoE in E-KO cells rescued infectious particle formation (Figure S2C, Figure S2D, Figure S2E). Next, to examine the redundant role of ApoB, the effect of knockdown of ApoB on HCV assembly was determined in parental and E-KO Huh7 cell lines (Fig. 2A). Knockdown of ApoB in E-KO cells resulted in a more efficient reduction of infectious particle production than that in parental Huh7 cells, suggesting that ApoB and ApoE have a redundant role in the formation of infectious HCV particles.

To further confirm the redundant role of ApoB and ApoE in the HCV life cycle, especially in the particle formation, 2 clones of ApoB and ApoE double-knockout (BE-KO1 and BE-KO2) Huh7 cells were established by ZFNs (Figure S3A and Figure S3B). The lack of ApoB and ApoE expressions was confirmed by immunoblotting and ELISA analyses (Figure S3C, Figure S3D, Figure

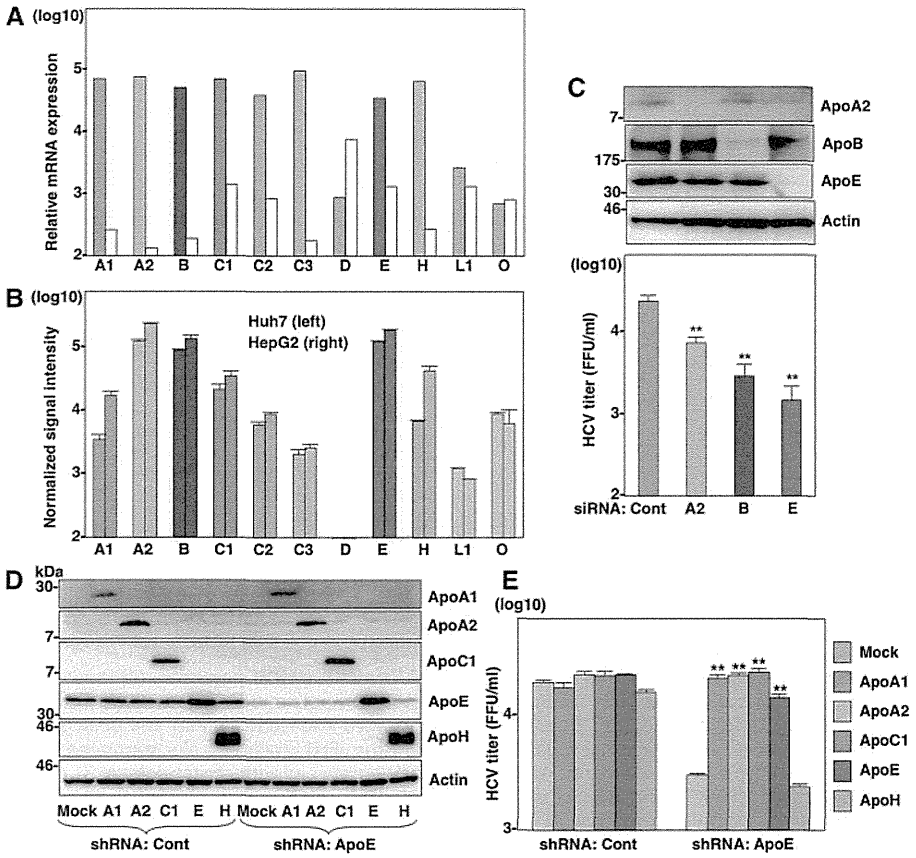

Figure 1. Several apolipoproteins participate in HCV propagation. (A) Relative mRNA expression of the apolipoproteins in the liver tissues (left columns) was determined using the NextBio Body Atlas application. The median expression (right columns) was calculated across all 128 human tissues from 1,068 arrays using the Affymetrix GeneChip Human Genome U133 Plus 2.0 Array. mRNA expression for each gene was log10 transformed. (B) Log10 transformed, normalized signal intensity of the apolipoproteins in Huh7 (left columns) and HepG2 (right columns) cells were extracted from previously published expression microarray dataset GSE32886. (C) Huh7 cells infected with HCVcc at an MOI of 1 at 6 h post-transfection with siRNAs targeting ApoA2 (A2), ApoB (B), ApoE (E) and control (Cont), and expression levels of apolipoproteins (upper panel) and infectious titers in the culture supernatants (lower panel) were determined by immunoblotting and a focus-forming assay at 72 h post-infection, respectively. (D) ApoA1, ApoA2, ApoC1, ApoE and ApoH were exogenously expressed in control and ApoE-knockdown Huh7 cells by lentiviral vectors. Expressions of the apolipoproteins were determined by immunoblotting analysis. (E) Infectious titers in the culture supernatants of control and ApoE-knockdown Huh7 cells expressing the apolipoproteins were determined by focus-forming assay at 72 h post-infection. In all cases, asterisks indicate significant differences (*, $P<0.05$; **, $P<0.01$) versus the results for control cells.
doi:10.1371/journal.ppat.1004534.g001

S3E). The BE-KO cell lines also exhibited no significant effect on the infectivity of HCVpp (Fig. 2B) and the colony formation of SGR (Fig. 2C). Next, we examined the redundant role of ApoB and ApoE on the propagation of HCVcc. Upon infection with HCVcc at an MOI of 1, infectious titers in the supernatants of BE-KO1 and BE-KO2 cells were 50 to 100 times lower than those of parental Huh7 cells at 72 h post-infection, while the level of intracellular RNA replication was comparable (Fig. 2D and E). In addition, exogenous expression of ApoE in BE-KO (ApoE-res) cells rescued the production of infectious viral particles to levels comparable to those in parental Huh7 cells (Fig. 2F and G), suggesting that ApoB and ApoE redundantly participate in the particle formation of HCV.

MTTP participates in HCV particle formation through the maturation of ApoB

It is difficult to determine the roles of ApoB in the particle formation of HCV, because ApoB is too large (550 kDa) to obtain cDNA for expression. However, previous reports have shown that expression of MTTP facilitates the secretion of ApoB [21]. To further clarify the roles of ApoB in the life cycle of HCV, we established knockout Huh7 cell lines deficient in MTTP (M-KO1 and M-KO2) and in both ApoE and MTTP (EM-KO1 and EM-KO2) by using the ZFN and CRISPR/Cas9 system (Figure S4A and Figure S4E). The lack of MTTP, ApoB and ApoE expressions was confirmed by immunoblotting and ELISA analyses (Figure Figure S4B, Figure S4C, Figure S4D, Figure S4F, Figure S4G, Figure S4H). As previously reported, the secretion of ApoB was completely abrogated in M-KO and EM-KO cells, while the mRNA levels of ApoB were comparable among Huh7, M-KO and EM-KO cells (Figure S4I). To examine the roles of MTTP in the assembly of HCV through the secretion of ApoB, HCVcc was inoculated into the Huh7, B-KO, M-KO, E-KO, BE-KO and EM-KO cell lines at an MOI of 1, and intracellular HCV genomes and infectious titers in the supernatants were determined (Fig. 3A–C). Although intracellular RNA replication in M-KO and EM-KO cells was comparable with that in Huh7, B-KO, E-KO and BE-KO cells (Fig. 3B), infectious titers in the supernatants of EM-KO cells were severely impaired as seen in BE-KO cells, while those of M-KO cells were comparable to those of parental Huh7cells (Fig. 3C), suggesting that MTTP participates

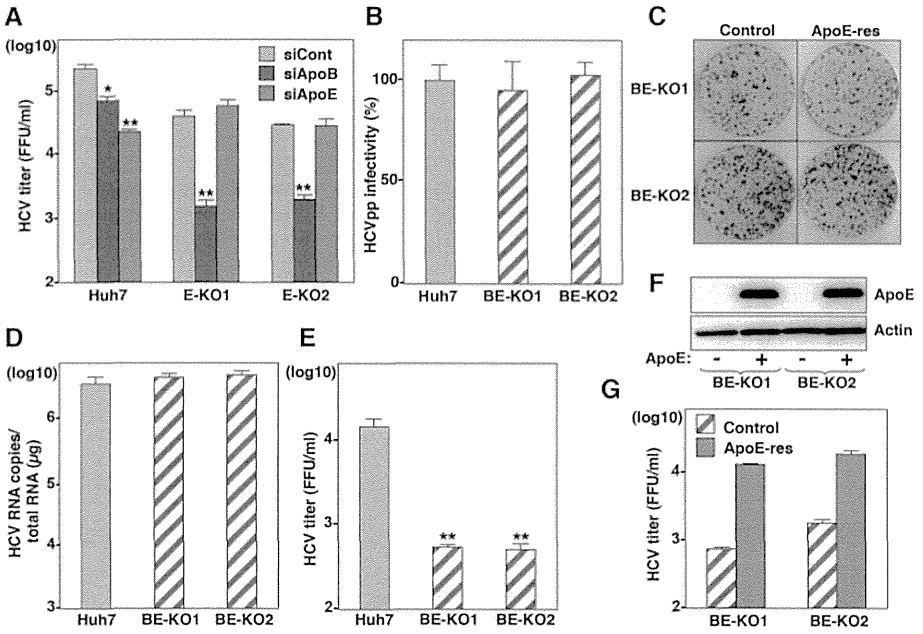

Figure 2. ApoB and ApoE redundantly participate in the formation of infectious HCV particles. (A) Huh7 and E-KO1 cells were infected with HCVcc at an MOI of 1 at 6 h post-transfection with siRNAs targeting ApoB or ApoE, and infectious titers in the culture supernatants were determined by focus-forming assay at 72 h post-infection. (B) HCVpp were inoculated into Huh7, BE-KO1 and BE-KO2 cells, and luciferase activities were determined at 48 h post-infection. (C) A subgenomic HCV RNA replicon of the JFH1 strain was electroporated into BE-KO1 and BE-KO2 cells with/without expression of ApoE by lentiviral vector (ApoE-res), and the colonies were stained with crystal violet at 31 days post-electroporation after selection with 400 μg/ml of G418. Huh7, BE-KO1 and BE-KO2 cells were infected with HCVcc at an MOI of 1, and intracellular HCV RNA (D) and infectious titers in the supernatants (E) were determined at 72 h post-infection by qRT-PCR and focus-forming assay, respectively. (F) Exogenous expression of ApoE in BE-KO1 and BE-KO2 cells by lentiviral vector was determined by immunoblotting analysis. (G) Infectious titers in the culture supernatants of BE-KO1 (gray bars) and ApoE-res cells (red bars) infected with HCVcc at an MOI of 1 were determined at 72 h post-infection by focus-forming assay.

doi:10.1371/journal.ppat.1004534.g002

in the HCV assembly through the regulation of ApoB secretion. To further confirm the roles of MTTP in HCV assembly through ApoB secretion, the effects of exogenous expression of MTTP in EM-KO cells on the infectious particle formation of HCV were determined. Immunoblotting and ELISA analyses revealed that exogenous expression of MTTP rescued the secretion of ApoB into the supernatants of EM-KO cells (Fig. 3D and E), while expression of ApoE or MTTP in both BE-KO and EM-KO cells exhibited no effect on the intracellular RNA replication (Fig. 3F). Although exogenous expression of ApoE rescued the infectious particle formation of HCV in both BE-KO and EM-KO cells, expression of MTTP rescued the particle formation in EM-KO cells but not in BE-KO cells (Fig. 3G), supporting the notion that MTTP plays a crucial role in the HCV assembly through the maturation of ApoB.

Exchangeable apolipoproteins redundantly participate in the assembly of infectious HCV particles

Next, to examine the roles played in HCV particles formation by other apolipoproteins highly expressed in the liver (Fig. 1A), the expressions of ApoA1, ApoA2, ApoC1, ApoC2, ApoC3 and ApoH in BE-KO1 cells were suppressed by siRNAs (Fig. 4A and Figure S5). While knockdown of ApoA1, ApoC3 and ApoH exhibited no effect, that of ApoA2, ApoC1 and ApoC2 significantly inhibited the release of infectious particles, which was consistent with the expression pattern of endogenous apolipoproteins except for ApoH in Huh7 cells (Fig. 1B), suggesting that not only ApoB and ApoE but also other exchangeable apolipoproteins participate in HCV particle formation. To confirm the redundant role of these apolipoproteins on the infectious particle formation, the effects of exogenous expression of these apolipoproteins on the propagation of HCVcc in BE-KO1 cells were determined. ApoA1, ApoA2, ApoC1, ApoC2, ApoC3, ApoE and ApoH were expressed by lentiviral vector in BE-KO1 cells (Fig. 4B upper panel). The expressions of ApoA1, ApoA2, ApoC1, ApoC2, ApoC3 and ApoE but not of ApoH enhanced extracellular HCV RNA, while they exhibited no effect on intracellular HCV RNA (Fig. 4C). In addition, the expressions of these exchangeable apolipoproteins enhanced the infectious particle formation in the supernatants of BE-KO1 cells (Fig. 4B lower panel). On the other hand, the expression of nonhepatic apolipoproteins, including ApoD, ApoL1, and ApoO, exhibited no effect on HCV particle formation in BE-KO1 cells (Figure S6). These results suggest that exogenous expression of not only the ApoE but also the ApoA and ApoC families can compensate for the impairment of HCV particle formation in BE-KO1 cells. Interestingly, specific infectivity (infectious titers/viral RNA levels in supernatants) was also enhanced by the expression of ApoA1, ApoA2, ApoC1, ApoC2, ApoC3 and ApoE, suggesting that these apolipoproteins participate in the infectious but not non-infectious particle formation of HCV (Fig. 4D). Previous reports have suggested that the expressions of Claudin1 (CLDN1), miR-122 and ApoE facilitate the production of infectious particles in nonhepatic 293T cells [16]. Therefore, the effects of exogenous expression of exchangeable apolipoproteins on particle formation were examined in 293T cells expressing CLDN1 and miR-122 (293T-CLDN/miR-122 cells). Exogenous expression of ApoA1, ApoA2, ApoC1, ApoC2, ApoC3 and ApoE, but not of ApoH by lentiviral vector facilitated the production of infectious